Taylor & Francis
Taylor & Francis Group

Separation & Purification Reviews

ISSN: 1542-2119 (Print) 1542-2127 (Online) Journal homepage: www.tandfonline.com/journals/lspr20

Sulfur-Enriched Biochar Derived from Waste Biomass: A Sustainable Soil Amendment?

Anna M. Kisiela-Czajka , Temifemi Agbebunmi , Krzysztof M. Czajka & Izabela Michalak

To cite this article: Anna M. Kisiela-Czajka , Temifemi Agbebunmi , Krzysztof M. Czajka & Izabela Michalak (08 Jun 2026): Sulfur-Enriched Biochar Derived from Waste Biomass: A Sustainable Soil Amendment?, Separation & Purification Reviews, DOI: 10.1080/15422119.2026.2680418

To link to this article: https://doi.org/10.1080/15422119.2026.2680418

Published online: 08 Jun 2026.

SEPARATION & PURIFICATION REVIEWS
https://doi.org/10.1080/15422119.2026.2680418

Sulfur-Enriched Biochar Derived from Waste Biomass: A Sustainable Soil Amendment?

Anna M. Kisiela-Czajka[a], Temifemi Agbebunmi[b], Krzysztof M. Czajka[a], and Izabela Michalak[b]

[a]Department of Energy Conversion Engineering, Faculty of Mechanical and Power Engineering, Wroclaw University of Science and Technology, Wroclaw, Poland; [b]Department of Advanced Material Technologies, Faculty of Chemistry, Wroclaw University of Science and Technology, Wroclaw, Poland

ABSTRACT

The review highlights the innovative use of biochar from diverse waste sources, including wood residues, agricultural and food waste, biosolids, municipal waste, and algae, for adsorbing sulfur compounds and its application as a soil fertilizer in agriculture. Biochar yields range from 17.6% (aloe-vera leaves, 500°C) to 65.4% (palm oil mill sludge, 300°C). High H_2S adsorption was observed with rice straw (1 g/g), eucalyptus (490 mg/g), and almond shells (230 mg/g), while sugarcane bagasse achieved a record 1.7 g/g for total sulfur adsorption from diesel. Oxidation of adsorbed gases releases sulfur as SO_4^{2-}, enhancing yields of corn (31–49%), soybeans (4–14%), and millet (115%). Sulfur-enriched biochar improves nutrient availability, water retention, enzyme activity, and organic matter, while lowering salinity, heavy metal (As, Hg) toxicity, and pathogen risk. Despite the sulfur-enriched biochar promise, validation in crop fields is needed. The lack of standards and limited research on fast pyrolysis, pressure, and feedstock optimization highlights critical gaps.

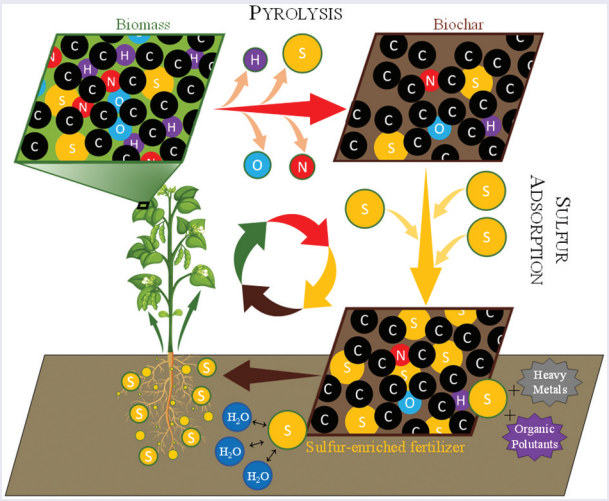

ARTICLE HISTORY
Received 1 April 2025
Revised 2 October 2025
Accepted 19 May 2026

KEYWORDS
pyrolysis; adsorption; sulfur-enriched biochar; circular economy; sustainable agriculture

INTRODUCTION

Emissions of sulfur compounds, in particular sulfur dioxide (SO_2) and hydrogen sulfide (H_2S), are a significant source of environmental acidification and air quality deterioration. Global SO_2 emissions primarily originate from the combustion of fossil fuels, specifically coal (~50%) and oil (~25%), as well as from industrial processes (~25%).[1] In the United States, SO_2 emissions peaked in 1973 and have been since then significantly reduced thanks to regulations such as the Clean Air Act and the Acid Rain Program. In China, emissions rose until the early 2000s and then fell by 75% after the introduction of the Air Pollution Prevention and Control Action Plan in 2013. SO_2 emissions have fallen particularly sharply in Europe: in the EU-27 countries, they decreased by around 80% between 1990 and 2021, while in the EEA-32 region (comprising 32 countries covered by the European Environment Agency), the decline was similar, at around 78% over the same period. These reductions were the result of restrictions on the sulfur content of fuels, the modernization of significant combustion sources (such as flue gas desulfurization installations), and the gradual

CONTACT Anna M. Kisiela-Czajka anna.kisiela-czajka@pwr.edu.pl Department of Energy Conversion Engineering, Faculty of Mechanical and Power Engineering, Wroclaw University of Science and Technology, Smoluchowskiego 21, Wroclaw 50-372, Poland; Izabela Michalak izabela.michalak@pwr.edu.pl Department of Advanced Material Technologies, Faculty of Chemistry, Wroclaw University of Science and Technology, Smoluchowskiego 25, Wroclaw 50-372, Poland

phase-out of coal-fired power plants. The most considerable reductions in emissions were recorded in Western European countries, while in some Eastern and Southern European countries, the process was slower, although still clearly visible.[2] In India, emissions have increased by 50% due to the growing use of coal, making the country the present world largest emitter of anthropogenic SO_2.[3] The release of sulfur-containing gases results in ecosystem degradation, soil and water acidification, accelerated corrosion of infrastructure, and an increased risk of respiratory diseases in humans. Even small, stationary sources of emissions, such as marginal oil wells, can lead to locally high concentrations of toxic gases – for example, in the Luling oil field (Caldwell County, Texas), H_2S emissions from active wells ranged from 0 to 5 g/h, with an average of 1.6 g/h or 47 mmol/h that are 1.1 L/h, which in practice means a local, constant source of toxic gas that can lead to dangerously high concentrations (above 100 ppm) in the vicinity of the wells,[4] posing a serious health risk to people in the area.

To date, regulatory and technological measures have enabled a significant reduction in sulfur emissions; however, the problem persists, particularly for sources that are dispersed. In industrial practice, three groups of conventional flue gas desulfurization methods dominate: wet, semi-dry, and dry. Although these technologies are well developed and capable of removing over 90% of SO_2, each has significant environmental and operational limitations.[5] Wet processes, of which the limestone-gypsum process is the most commonly used, require very high investment and operating costs, high water consumption, and generate wastewater containing reaction products that require further treatment.[6] Semi-dry and dry methods reduce water consumption but generate large amounts of solid reaction waste – mixtures of unreacted sorbent, fly ash, and sulfates – whose disposal or management is costly and logistically challenging.[7] All these technologies are also characterized by low flexibility, as they are designed for a strictly defined flue gas composition and process parameters, which makes it challenging to adapt them to variable operating conditions and smaller installations.

Although global SO_2 and H_2S emissions are declining,[8] challenges persist for smaller emission sources and specialized, dispersed industries, including pulp and paper, small power plants, and local industrial boiler rooms. This necessitates not only further refinement of proven emission reduction technologies, but also the development of more operationally flexible, cost-effective, and circular economy-compliant solutions that can effectively reduce sulfur emissions even from dispersed and difficult-to-control sources. This opens up space for alternative and resource-efficient solutions, such as biochar that appears to be an alternative with high potential. Thanks to its large specific surface area, high porosity, thermal stability, and the presence of diverse functional groups, it enables the effective binding of SO_2, H_2S, and other gaseous pollutants at relatively low operating costs.[9,10] Laboratory tests have shown that iron-impregnated maple biochar (MB-Fe) achieves a maximum H_2S adsorption capacity of 23.9 mg/g, which is a 3.9-fold increase compared to unmodified maple biochar (MB, 6.1 mg/g). Similarly, iron-impregnated corn stalk biochar (CSB-Fe) achieves a capacity of 8.2 mg/g, which is 2.5 times higher than unmodified biochar from the same raw material (CSB, 3.3 mg/g).[11] The H_2S capacities of biochar are lower than those of some commercial chemical sorbents, which can reach 667 mg/g for activated carbon produced from charcoal, chemically activated with phosphoric acid and modified with metal salts, 20–40 mesh grain size.[12] Biochar produced from waste biomass offers significant benefits in terms of sustainability. Its low production costs and flexibility in adapting to different emission sources make it an attractive and environmentally friendly alternative to synthetic sorbents. Additionally, its ability to be reincorporated into the material cycle enables the combination of emission reduction with agricultural practices, aligning with the concept of a closed-loop economy. Notably, biochar produced from waste biomass not only reduces pressure on primary raw materials but also facilitates the management of organic waste streams. Unlike conventional sorbents, used biochar can, after environmental safety assessment, be reused as a soil additive, providing sulfur as an essential micronutrient and improving the physicochemical properties of the substrate. This "resource-oriented" approach transforms the problem of secondary waste into a value-added product by integrating the reduction of sulfur emissions with agricultural practices and implementing the key principles of the circular economy and sustainable development.[13–15]

The properties of biochar can be deliberately modified by selecting specific parameters of the production process, such as pyrolysis temperature, heating rate, residence time in the reactor, type of biomass, as well as the degree of grinding and drying of the raw material, which enables the optimization of its sorption capacity. Although there are many studies in the literature devoted to the characteristics of biochar and its sorption properties,[16] there is still a lack of systematic analyses of the impact of fast and flash pyrolysis, overpressure conditions, and optimization of raw material preparation, including grinding and drying, on the properties of the final product. Also, the available sources still do not provide systematic information on the possibility of reusing biochar after the adsorption process, especially in agricultural applications as a sulfur carrier and an agent for supporting soil physicochemical properties. A literature review with Scopus, keywords "reuse" AND "spent" AND "adsorbent," showed that only seven papers on spent sorbent management were published between 2015 and 2025, of which only a few concerned agricultural applications. The study by Hu et al.[17] demonstrated the effectiveness of spent adsorbents in removing micropollutants from wastewater, while Fouda-Mbanga et al.[18] confirmed their efficiency in extracting heavy metals. The potential for their revalorization in forensic science was presented by Nthwane et al.[19] The use of spent adsorbents as additives in cement and ceramic materials was discussed in[20] and,[21] whereas their impact on the firing process of clay bricks was analyzed in.[22] Additionally, Arunachellan et al.[23] described their application as catalysts in phenol reactions.

These scattered findings highlight that, despite growing interest in biochar adsorption, systematic knowledge on the reuse of spent sorbents – particularly in agriculture – remains scarce. This gap highlights the need for integrated research. It

provides a unique perspective, which is the focus of the present review, specifically on the "resource-oriented" application of sulfur-enriched biochar in agriculture.

KEY BIOMATERIALS FOR EFFECTIVE SULFUR REMOVAL

The selection of suitable material for biochar production is crucial for both the efficiency of its production and its subsequent use in sulfur compound removal processes. This analysis evaluated various sources of waste biomass in terms of their suitability for biochar production and their ability to adsorb sulfur compounds such as H_2S and SO_2. Six main groups of biowaste were selected for the study: agricultural waste, wood waste, food waste, bio-solid waste, municipal waste, and algae (Table 1). The biochar yield varies widely, ranging from 17.6% for aloe-vera leaves at 500°C[30] to 65.4% for palm oil mill sludge at 300°C.[44] High yields were also achieved for rice hull (41.9% at 400°C),[24] banana peels (39.5% at 400°C),[24] banana empty fruit bunch (29.3% at 350°C)[29] and almond shells (28.0% at 500°C).[33] Although the microalgae *Sargassum* sp. exhibited a biochar yield of 30.2%,[46] they required significantly higher pyrolysis temperatures of 800°C. Compared to the above examples, from a practical point of view, pyrolysis at 800°C is an energy-intensive and costly process. With an adsorption efficiency of H_2S at 5.80 mg/g, *Sargassum* sp. is not the optimal material. The lowest biochar yields were recorded for palm oil sewage sludge (5.43% at 400°C),[44] aloe leaves (17.6% at 500°C)[30] and used coffee grounds (18.9% at 500°C).[30] Unfortunately, in many cases, authors did not provide information on the biochar yield, particularly for biochar derived from agricultural waste, which complicates a complete assessment of these material potential.

It is worth noting that the pyrolysis temperature has a significant impact on biochar yield, as clearly illustrated by the results presented in.[24] For banana peels, the yield decreased from 39.5% at 400°C to 28.2% at 600°C, for rice hulls from 41.9% to 30.1%, and for sawdust from 29.4% to 22.6%. These results reflect a commonly observed trend in which higher temperatures intensify the degradation of cellulose and hemicellulose, promoting further degassing of the carbon structure and resulting in a decrease in yield.[48,49] However, the scale of this phenomenon depends on the type of biomass, which is related to its chemical composition. Biomass rich in cellulose and hemicellulose, such as soft agricultural waste (e.g., banana peels) or rice husks, achieves high yields at lower temperatures but shows a 28% decrease in efficiency compared to the initial value as the temperature increases. On the other hand, lignin-rich biomass, such as sawdust or eucalyptus, is more resistant to thermal degradation, resulting in more stable yield values, although with a 23% downward trend. In addition, the minimal differences in biochar yield were observed for banana peels in the temperature range of 550–600°C, decreasing of only 5%. It may be due to the intensive degradation of the remaining cellulose and hemicellulose and the rapid release of volatile components. In the case of straw and rice husks, the decrease in efficiency is more uniform, probably due to the higher thermal stability of lignin in these raw materials. It should be noted that despite the common trend of yield reduction, absolute values remain diverse – for example, rice hulls achieve a higher yield than sawdust even at higher temperatures. This phenomenon highlights the key role of the proportions of lignin, cellulose, and hemicellulose in determining the process efficiency. It indicates the need for individual selection of pyrolysis parameters based on the biomass characteristics.

Regarding selected biological waste, it is essential to note that its primary application is the adsorption of H_2S. Biochar from rice straw, modified with copper and obtained by pyrolysis at 600°C, showed the highest H_2S adsorption capacity – 1 g/g.[28] The best adsorption properties were observed for the sample, which, after copper impregnation, was calcined at 300°C. Compared to the sample calcined at 200°C, this material had a larger specific surface area (36 m^2/g vs. 24 m^2/g) and a higher oxide content (1.5% vs. 0.5%). At 25°C, this material had a greater number of active sites capable of H_2S chemisorption. In addition, adsorption at 120°C promoted the formation of stable chemical bonds between H_2S and the biochar surface, resulting in an extended breakthrough time of 400 minutes.

In terms of H_2S adsorption efficiency, the best results were obtained for rice husks (94.7%), sawdust (95.0%), and banana peels (98.2%).[24] However, it should be noted that these results are given as percentages without specifying the initial concentration of the sulfur compound. This method of presentation renders it impossible to convert the data into a standard mg/g adsorption capacity, which hinders direct comparison of the effectiveness of different materials and assessment of their efficiency at varying gas concentrations. Biochar from rice husks (RHB-500) showed the presence of key functional groups, including O–H, N–H, and C=C. The material was characterized by a heterogeneous surface, including pores with a diameter of approximately 21.3 μm and micropores <30 μm formed during pyrolysis. This type of disordered structure increases the total sorption surface area, but at the same time may limit the efficiency of gas transport to active adsorption sites. Biochar from sawdust (SDB-500) exhibited a similar set of functional groups (O–H, C–O, C=C, Si–O–Si). Still, its structure was more ordered, with a honeycomb character, a layered arrangement of pores with a diameter of ~13.7 μm, and micropores <30 μm. This porosity facilitated more efficient transport of H_2S to active sites, which may explain the slightly higher sawdust adsorption efficiency compared to biochar from rice husks. In the case of both materials, the high pyrolysis temperature led to dehydration and partial decomposition of the –OH groups, thereby affecting the availability of reactive chemisorption centers. Biochar from banana peels was distinguished by its longitudinal fibrous structure, resulting from the natural structure of the raw material. The average pore diameter was 13.8 μm, comparable to that of sawdust. The material retained a relatively larger number of reactive hydroxyl groups from alcohols and carboxylic acids, even after pyrolysis at 550°C. The fibrous and orderly structure

Table 1. Comparison of waste biomass-derived biochars for sulfur compound removal.

Raw material / its form	Pyrolysis / Operation conditions	Pyrolysis yield (%)	Form of sulfur removed by biochar	Sulfur removal by activated biochar*	Ref.
1. Agricultural waste					
Rice hull / ground and sieved form	400, 450, 500, 550, 600°C, 10°C/min, 4 h	from 41.9 (at 400°C) to 30.1 (at 600°C)	H_2S from municipal solid waste	94.7%# (*for biochar obtained at 500°C)	[24]
Dairy manure / ground and sieved form	700°C, h.r. – n.a., 6 h	n.a.	SO_4^{2-} from sodium sulfate solution	3.7 mg/g	[25]
Sugarcane bagasse / sieved form	700°C, h.r. – n.a., 4 h, melamine-functionalized biochar with magnetic $CuFe_2O_4$	n.a.	total sulfur from diesel fuel	1.7 g/g	[26]
Cow dung / dried form	500, 650, 750°C, 20°C/min, 60 min	n.a.	H_2S from biogas	38.2 mg/g (*650°C)	[27]
Pig manure / dried form	500, 650, 750°C, 20°C/min, 60 min	n.a.	H_2S from biogas	16.5 mg/g (*750°C)	[27]
Chicken manure / dried form	500, 650, 750°C, 20°C/min, 60 min	n.a.	H_2S from biogas	4.9 mg/g (*750°C)	[27]
Coconut husk / dried form	500, 650, 750°C, 20°C/min, 60 min	n.a.	H_2S from biogas	38.7 mg/g (*750°C)	[27]
Rice straw / powdered form	600°C, 20°C/min, 60 min, steam-activated Cu-modified biochar	n.a.	H_2S from gas streams	1 g/g	[28]
Banana empty fruit bunch / ground and sieved form	350°C, h.r. – n.a., 4 h	29.3	H_2S from gas streams	7.7 mg/g	[29]
Corn cob / powdered form	500°C, h.r – n.a., 2 h	23.0	H_2S from biogas	47 mg/g	[30]
2. Wood residue					
Sawdust / ground and sieved form	400, 450, 500, 550, 600°C, 10°C/min, 4 h	from 29.4 (at 400°C) to 22.6 (at 600°C)	H_2S from municipal solid waste	95%# (*500°C)	[24]
Camphor tree / ground and sieved form	100, 200, 300, 400, 500°C, 10°C/min, 5 h	n.a.	H_2S from the exhaust gas	1.2–121 mg/g (*400°C)	[31]
Used wood pallet / sieved form	700°C, 22°C/min, 30 min	n.a.	H_2S from dry syngas	13 mg/g	[32]
Eucalyptus / ground and sieved form	500°C, h.r. – n.a, r.t. – n.a, KOH-activated pyrolyzed biochar	36	H_2S from biogas	490 mg/g	[33]
Almond shells / ground and sieved form	500°C, h.r. – n.a, r.t. – n.a., KOH-activated pyrolyzed biochar	28.5	H_2S from biogas	230 mg/g	[33]
Commercial pinewood chip / particle form	456, 500, 600°C, h.r. – n.a., 10 h	n.a.	H_2S from livestock environment	2.5 mg/g (*465°C)	[34]
Black spruce / ground form	454°C, h.r. – n.a., r.t. – n.a., further activation in the presence of CO_2 at 900°C	n.a.	SO_2 from industrial activity	25 mg/g	[35]
White birch / ground form	454°C, h.r. – n.a., r.t. – n.a., further activation in the presence of steam at 900°C	n.a.	SO_2 from industrial activity	76.9 mg/g	[35]
3. Food waste					
Orange waste / ground and sieved form	400*, 600°C, 5°C/min, r.t. – n.a.	25.5 at 400°C	H_2S from waste cooking oil	78.3%# (*400°C)	[36]
Banana peel / ground and sieved form	400, 450, 500, 550, 600°C, 10°C/min, 4 h	from 39.5 (at 400°C) to 28.2 (at 600°C)	H_2S from municipal solid waste	98.2%# (*550°C)	[24]
Orange pruning / powdered form	400, 600°C, 10°C/min, r.t. – n.a.	n.a.	H_2S from waste cooking oil	78.8%# (*600°C)	[36]
Potato peel waste / crushed and sieved form	500°C, h.r. – n.a., 5 min	n.a.	H_2S from stream gas	53 mg/g	[37]
Oil palm fiber / ground and sieved form	450°C, 12°C/min, 98 min	24.4	SO_2 from power plants	18.6 mg/g (*450°C)	[38]
Coffee grains / ground and sieved form	500°C, 10°C/min, 3 h	23.0	H_2S from biogas	22 mg/g	[33]
Coffee industry waste / pelleted form	500, 600, 700, 800°C, 10°C/min, 3 h	n.a.	H_2S from stream gas	281.5 mg/g (*500°C)	[39]
Spent coffee / powdered form	500°C, h.r. – n.a., 2 h	18.9	H_2S from stream gas	66.3 mg/g	[30]
4. Bio-solid waste					
Sewage sludge / ground and sieved form	300°C, h.r. – n.a., 11 h	n.a.	H_2S from biogas	43.9%#	[40]
Palm oil sludge	300, 442, 700°C, 20°C/min, 30–150 min	n.a.	SO_2 from flue gas	16.7 mg/g (*442°C)	[41]
Activated sludge char / particle form	Microwave-assisted pyrolysis and physical activation; 500, 600, 700°C, h.r. – n.a., r.t. – n.a.	n.a.	H_2S from stream gas	9.15 mg/g (*500°C)	[42]
Sludge–margin mixture	400, 500°C, h.r. – n.a., – 4 h	n.a.	H_2S from biogas	97.0%# (*500°C)	[43]

(*Continued*)

Table 1. (Continued).

Raw material / its form	Pyrolysis / Operation conditions	Pyrolysis yield (%)	Form of sulfur removed by biochar	Sulfur removal by activated biochar*	Ref.
Palm oil mill sludge / ground form	300, 400, 500 C, 10–20°C/min, 60–120 min	from 65.4 (at 300°C, 20°C/min) to 41.8 (at 500°C, 10°C/min)	SO_2 from the combustion of fossil fuel or waste incineration	10 mg/g (*400°C)	[44]
5. Municipal waste					
Leaf waste / ground and sieved form	200, 300, 400°C, h.r. – n.a., r.t. – n.a.	n.a.	H_2S from biogas	8.4 mg/g (*400°C)	[45]
Aloe-vera leaves / powdered form	500°C, h.r. – n.a., 2 h	17.6	H_2S from biogas	106 mg/g	[30]
6. Algae waste					
Sargassum sp. / powdered form	400, 600, 800°C, h.r. – n.a., 20 min	30.2 at 800°C	H_2S from biogas	5.80 mg/g (*800°C, 200 ppm inlet)	[46]
Enteromorpha sp. / powdered form	400, 600, 800°C, h.r. – n.a., 20 min	26.1 at 800°C	H_2S from biogas	0.65 mg/g (*800°C, 1500 ppm inlet)	[46]
Chlorella sp. / powdered and sieved form	800°C, h.r. – n.a., 20 min	n.a.	H_2S from a gas cylinder	96.1 mg/g	[47]
Spirulina sp. / powdered and sieved form	800°C, h.r. – n.a., 20 min	n.a.	H_2S from a gas cylinder	69.4 mg/g	[47]

n.a – not available, * – the best pyrolysis temperature to obtain the highest sulfur compounds removal.
h.r. – heating rate, r.t. – residence time.
- values presented as in the original article, not recalculated.

facilitated mass transport and H_2S contact with the surface, resulting in the highest adsorption efficiency among the tested materials. Additionally, some of the C=O groups underwent aromatization during pyrolysis, potentially increasing the surface chemical activity.

Biochar from sugarcane bagasse, modified with $CuFe_2O_4$ nanoparticles and functionalized with melamine (Me-BC/$CuFe_2O_4$), exhibited exceptional adsorption capacity for SO_2, reaching 1.7 g/g at 700°C.[26] The N–H band confirmed the presence of nitrogen in the material structure at 3487 cm^{-1}, while the characteristic Cu–O peaks (402 and 593 cm^{-1}) indicated the preservation of the $CuFe_2O_4$ spinel structure. Raman analysis revealed an I^D/I^G ratio of ≈ approximately 0.98, indicating an increased number of defects in the graphite structure resulting from the functionalization and delamination of the biochar sheets. The material was also characterized by a high 361 m^2/g specific surface area, compared to 62.4 m^2/g for unmodified biochar, and a mesoporous structure with a pore diameter of ~15.9 nm, providing a large number of active adsorption sites. The porosity was irregular, with visible voids and channels, and $CuFe_2O_4$ nanoparticles were evenly distributed on the surface of the biochar. TEM images revealed dark spots corresponding to nanoparticles deposited on melamine-functionalized sheets, further highlighting the high efficiency of the material in adsorbing sulfur gases.[26]

Although biochar yield increases with decreasing pyrolysis temperature,[24] establishing a clear relationship between pyrolysis temperature and sulfur compound adsorption efficiency is challenging (Figure 1), as the properties of the feedstock strongly influence the outcome. Among the analyzed waste groups, both more mineral-rich and lignocellulosic feedstocks are present. It has been observed, however, that pyrolysis temperatures passing 500°C favor biochars derived from lignocellulosic materials, such as agricultural waste (sugarcane bagasse, rice straw, and banana empty fruit bunch) and wood residue (eucalyptus and camphor tree), for which the maximum sulfur adsorption exhibits a linear dependence on the biochar production temperature within the range of 300 to 900°C. In contrast, organomineral feedstocks, such as chicken manure or pig manure, exhibit significantly lower adsorption efficiency, regardless of the pyrolysis temperature.

BIOCHAR PRODUCTION AND MODIFICATIONS FOR ENHANCED SULFUR REMOVAL EFFICIENCY

The publications summarized in Table 1 were reviewed to assess the various technologies employed in producing biochar to remove gaseous sulfur compounds. The review focused on several aspects, including the method of feedstock preparation, such as whether and how the material was dried, as well as the grain size distribution used for pyrolysis. It also covered details

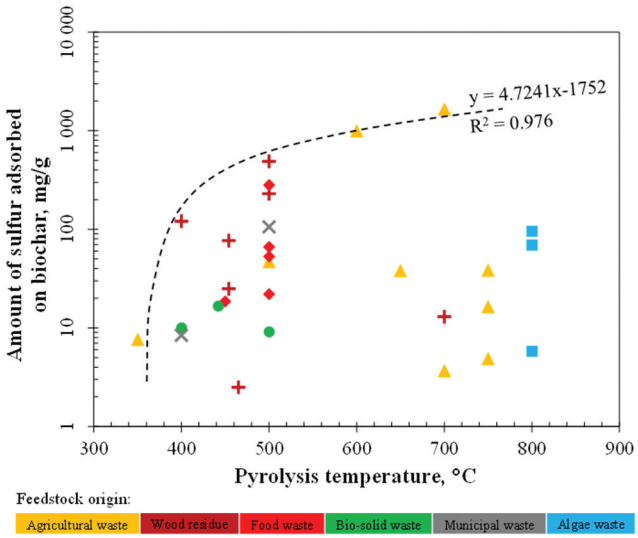

Figure 1. Relationship between the pyrolysis temperature of biowaste and the sulfur compounds adsorption capacity of biochar.

of the pyrolysis process, including the reactor type, sample mass, carrier gas flow rate, heating rate, temperature, residence time, atmosphere composition, and pressure. Lastly, the analysis examined whether the produced biochar underwent additional processing, such as activation or separating specific fractions to remove sulfur compounds.

Feedstock Preparation

The moisture content in the feedstock is known to increase the energy requirements for the pyrolysis process, as a significant portion of the energy is used for evaporation.[50] However, moisture evaporation also promotes the development of biochar porosity. Additionally, the steam released during this process contributes to the production of hydrogen-rich fuel gas by enhancing the steam reforming of volatiles and the steam gasification of biochar.[51–53] In 21 of the 24 studies listed in Table 1, the feedstock was dried to eliminate nearly all inherent and surface moisture, using widely differing methods. Sanchez-Borrego et al.[36] dried the waste biomass in an oven at 45°C as part of a two-stage process, but the duration was not specified. Sun et al.[37] and Shang et al.[31] thermally dried their material at 60°C for 24 and 48 h, respectively. Su et al.[27] dried the material at 65°C for 24 h, while Sahota et al.[45] used 75°C overnight. Baikousi et al. [30] and Juntarachat and Onthong[29] dried their samples at 80°C for 24 h. Higher temperatures were also employed in later studies, including 100°C overnight,[46] 100°C for 24 h,[24] 105°C for 24 h[33,38,44] and 110°C overnight.[26] In the case of the 12 analyzed studies, detailed information was provided regarding both the temperature and the duration of the drying process. Interestingly, as shown in Figure 2, it can be observed that in more than 66% of these studies, the fuel drying time was 24 h regardless of the process temperature, which indicates that it was not optimized.

An alternative method, which involves removing only a portion of the moisture, was employed in the studies.[32,43] In Gaga et al.[43] the feedstock was maintained at a moisture level of 20%, whereas Hervy et al.[32] maintained it at 30%. Xu et al.[42] employed a unique approach by completely drying some of the material at 105°C, while other portions were dried to moisture contents of 15% and 30%. Additionally, the literature review revealed two studies[35,39] in which pyrolysis was performed on feedstocks in their original condition as received, without reported information on moisture content. The second crucial factor in biochar production is the size of the feedstock particles used in the pyrolysis. Although grinding the material to achieve smaller particle sizes is energy-consuming, it significantly shortens the pyrolysis time. As with drying, the literature review reveals many methods to accomplish this. In some of the studies analyzed, the feedstock was not subjected to grinding. The biochar produced in this way was derived from sewage plant sludge,[43] banana peel and banana empty fruit bunch waste,[29] leaf waste biomass collected from in-house vegetation,[45] various types of livestock manure and coconut husk.[27] In one study,[39] the coffee industry waste used for pyrolysis was not only unground but was also fed into the reactor in pellet form.

Other authors subjected the feedstock to grinding and sieving to obtain specific particle size fractions, as shown in Figure 3. In the study by Iberahim et al.[44] biochar was produced from palm oil mill sludge that was ground and sieved to a fine particle size in the range of 300–500 mm, while in another study by the same authors,[38] oil palm fiber was processed with a particle size range of 100–300 mm. Hervy et al.[32] chipped wood pallets into particles with an average diameter of 30 mm. Feedstocks with a maximum grain size of 2 mm were subjected to pyrolysis by Sahota et al.[45] Izhar et al.[24] and Junior and Guo.[40] In comparison, Sanchez-Borrego et al.[36] and Xu et al.[42] used a maximum size of 1 mm. In the study by Shang et al.[31] three different fractions were analyzed: particles in the 0.4–1.25 mm range, those in the 0.3–0.4 mm range, and particles smaller than 0.3 mm. Sun et al.[37] pyrolyzed materials with a size range of 0.15–0.45 mm and Dou et al.[47] used particles below 0.3 mm. The feedstocks with the smallest particle sizes used for biochar production included dairy manure, with a maximum size of 0.18 mm,[25] as well as coffee grains, eucalyptus bark and almond shells,[33] which had particle sizes ranging from 0.11 to 0.25 mm.

As indicated by the cited studies, there are no widely accepted standards specifying the optimal form in which materials should be subjected to pyrolysis. The cited works provide little discussion on the rationale for fuel grinding or on the influence of particle size on the energy demand of the process and the properties of the resulting biochar. Consequently, the feedstocks used for pyrolysis vary greatly, ranging from finely ground samples with a maximum particle diameter of less than 0.18 mm, to coarsely ground materials with particle sizes of several to several dozen mm, to as-received feedstocks, and even pelletized forms. In addition to drying and grinding, feedstock materials were sometimes subjected to preliminary washing to remove impurities. Han et al.[46] washed fresh macroalgae with water five times, when Sahota et al.[45] washed only twice a leaf waste mixture. In the following studies, detailed information about the washing process was not

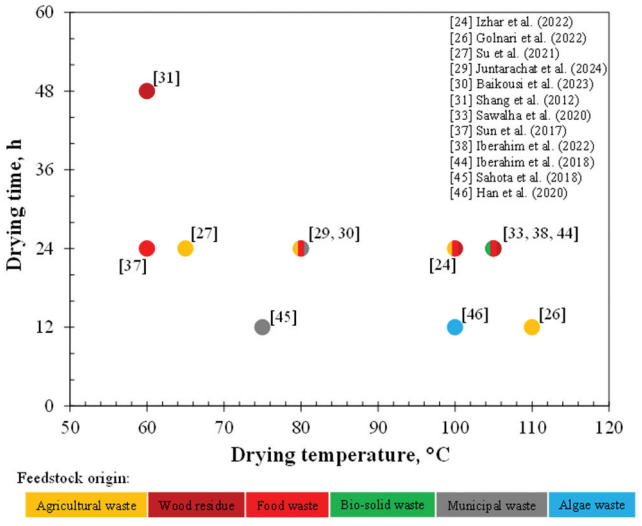

Figure 2. The relationship between the bio feedstock drying time and drying temperature.

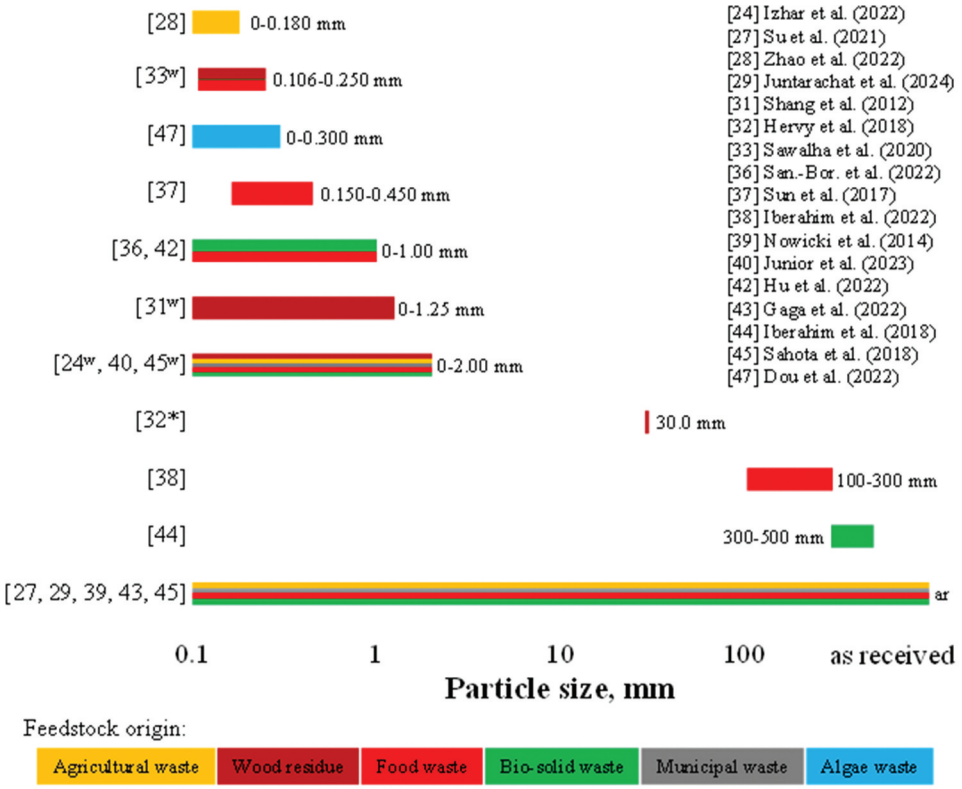

Figure 3. Particle size of the feedstock subjected to drying. Symbols: * – average particle size; w – materials subjected to preliminary washing.

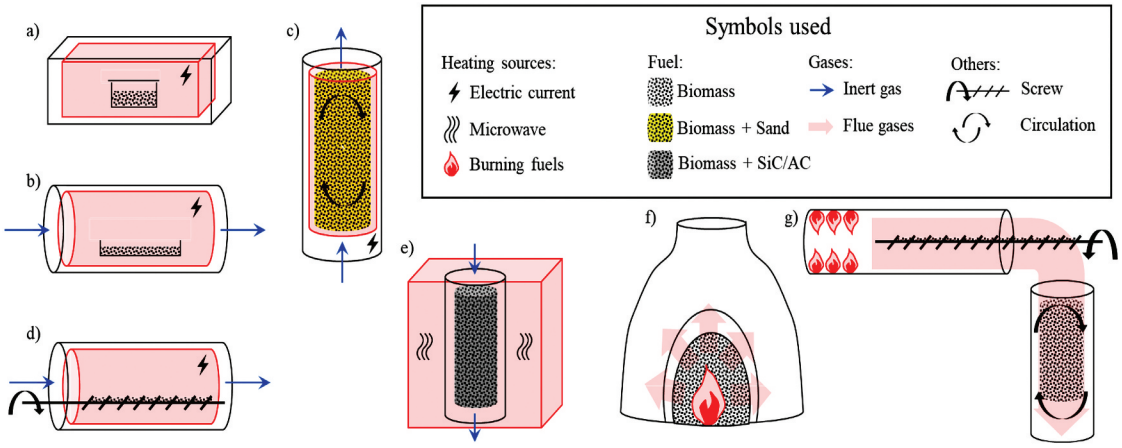

Figure 4. Reactor designs used for biochar production. Symbols: (a) muffle furnace; (b) tubular batch reactor; (c) fluidized bed reactor; (d) semi-continuous screw reactor; (e) microwave quartz tube; (f) traditional kiln; (g) cyclonic bed reactor.

provided. Still, it is known that it was applied to materials such as rice hulls, banana peels and sawdust,[24] camphor tree branches,[31] coffee grain waste, eucalyptus bark and almond shells.[33]

Pyrolysis Conditions

The feedstock materials, once properly prepared, underwent pyrolysis in reactors that varie significantly in design and function. The designs of the most commonly used reactors are presented in Figure 4. One of the most common methods involved placing the material in lidded crucibles and heating them in a muffle furnace[24,25,33] (see Figure 4a). Since the crucibles were tightly sealed, no oxygen or water vapor could enter from outside, resulting in a limited oxygen environment where the material only interacted with the oxygen trapped inside the crucible. This experimental setup is akin to the standard procedure for measuring volatile matter content in proximate analysis, such as ASTM Standard D1762-84. Although this approach is simple and repeatable, it subjects the biochar to secondary pyrolysis reactions, as the gases released during the process remain in contact with the biochar throughout. Even though it is rarely specified, only a small amount of material – just a few grams – is likely processed per

batch using this method. An adaptation of the method mentioned above was introduced by Junior and Guo,[40] who substituted the porcelain crucibles with a metal canister. This canister features a 5 mm hole in the lid, enabling the release of pyrolysis gases and thereby reducing the effect of secondary pyrolysis. With an internal diameter of 110 mm and a height of 130 mm, the container can accommodate larger sample volumes.

Another widely used approach to biochar production involves the use of a tubular reactor,[26,27,30,36,44,47] as shown in Figure 4b. This method is also a batch process in which the sample is placed inside a reactor flushed with an inert gas, and the temperature is controlled through electric heating. This method effectively prevents secondary pyrolysis, but gas flushing can introduce some inaccuracy in measuring the actual bed temperature of the material. The reactors employed can be oriented either horizontally[26] or vertically,[36] with generally consistent dimensions, typically featuring an internal diameter of 30–40 mm and a height of 160–500 mm.[27,36,38,44] Nitrogen is the inert gas most frequently used,[26,27,36,38,44,47] although argon is also sometimes utilized.[30] Carrier gas flow rates vary from 30 to 300 mL/min,[36,44,47] and processed material typically weighs a few grams, ranging from just over 4 g [36] to about 10 g.[26,38,44] Similar pyrolysis conditions to those in a tubular reactor, where the material sample is flushed with an inert gas in a bed, can also be replicated using a controlled atmosphere muffle furnace, as demonstrated by.[31]

Sun et al.[37] proposed an alternative method for biochar production, employing a fluidized bed reactor preloaded with a material mixture and 5 g of sand, shown in Figure 4c. The spatial velocities applied ranged from 700 to 8000 L/h. In contrast, Hervy et al.[32] used a semi-continuous horizontal screw reactor with a diameter of 167 mm and a length of 2000 mm to produce biochar (Figure 4d). Xu et al.[42] took a different approach, using a vertical microwave quartz tube with an inner diameter of 15 mm and a length of 270 mm, which was purged with nitrogen. To address the poor microwave absorption of the sludge, it was mixed with materials with strong microwave absorption properties, such as activated carbon and silicon carbide (SiC), as presented in Figure 4e. The mixture was then heated to the target temperature using a microwave with a constant power of 800 W. The literature review also highlighted efforts to produce biochar from waste biomass using large-scale methods, such as a traditional kiln[45] and the commercially available cyclonic bed reactor (CarbonFX technology),[35] shown in Figure 4f,g, respectively. Of all the studies reviewed, only Braghiroli et al.[35] employed fast pyrolysis, whereas the others[24,27,30–32,36,43,44] utilized slow heating, with rates ranging from 5 to 22°C/min. The absence of studies addressing the application of biochars derived from fast and flash pyrolysis for sulfur removal constitutes a significant knowledge gap and is particularly notable given the widespread industrial deployment of these techniques.

Figure 5 illustrates the relationships between the applied heating rate, residence time, and temperature for slow pyrolysis, showing results only for studies that reported all three variables in detail. Process temperatures varied from 100°C[31] to 800°C.[39,44,46,47] The temperature of 500°C was the most commonly used, appearing in 11 studies, while 400 and 600°C

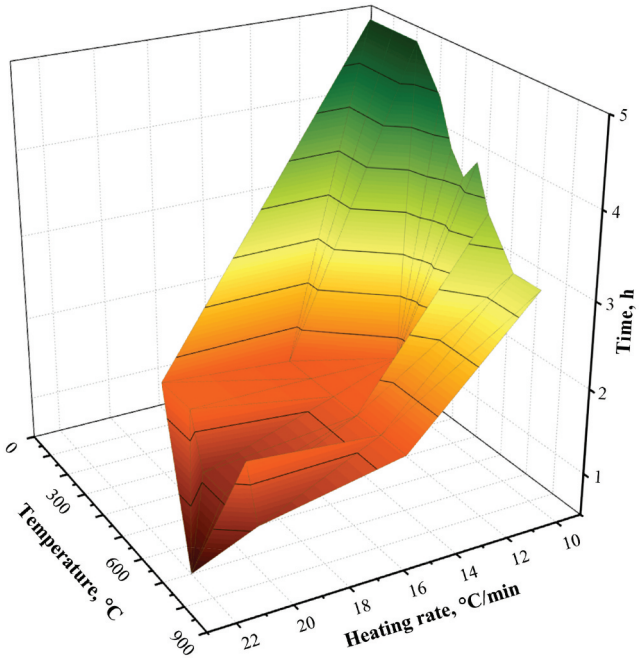

Figure 5. Relationships between heating rate, residence time and temperature in slow pyrolysis.

were each used in 8 studies. The residence times in the reactor varied considerably, ranging from 5 minutes[37] to approximately 11 h [40] (not included in the figure due to missing information on the heating rate). In most cases, the process took no more than several hours. The results presented in Figure 5 indicate that lower heating rates are generally associated with shorter residence times. This relationship can be attributed to the fact that reduced heating rates prolong the non-isothermal stage of pyrolysis, thereby enhancing the extent of biochar carbonization and increasing its yield.[54] In contrast, extending the residence time at elevated temperatures would be inefficient, as it promotes further decomposition of the solid phase, consequently decreasing the biochar yield. Notably, only one study[37] investigated biochar production under mild overpressure conditions, whereas all other studies[24–27,30,38] conducted pyrolysis at atmospheric pressure. The influence of pressure on the sulfur sorption capacity of biochar and its suitability as a soil amendment remains a critical and strikingly understudied knowledge gap. Pressurized pyrolysis emerges as a promising strategy, offering the potential to increase biochar yield, achieve precise control over its physicochemical properties, and mitigate the environmental impacts of the process.

Post-Pyrolysis Treatments and Modifications

Typically, the biochar produced was not sieved, and the whole material was used for sulfur compounds removal.[31,33,36–41,43,44,46] However, as shown in Figure 6, some researchers have chosen specific particle size fractions of the biochar. Golnari et al.[26] used particles smaller than 2 mm, Braghiroli et al.[35] selected fractions of 1–2 mm, Hervy et al.[32] used sizes between 0.5 and 1.6 mm, Juntarachat and Onthong[29] and Xu et al.[42] focused on

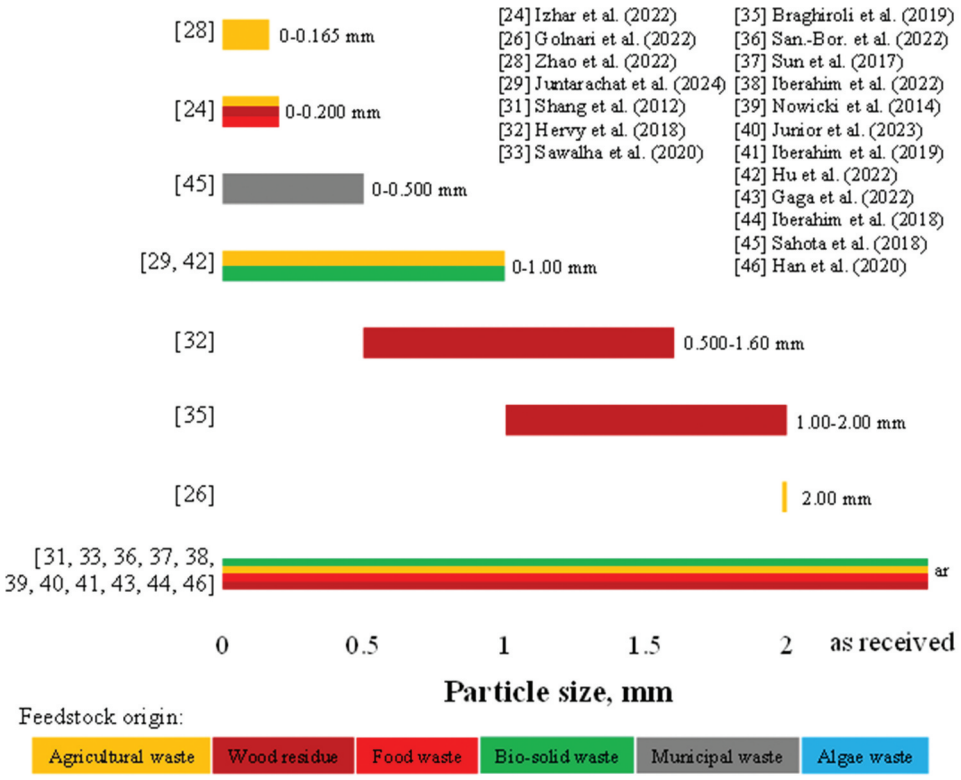

Figure 6. Particle size of biochars used for the removal of sulfur compounds.

fractions smaller than 1 mm, Sahota et al.[45] used particles smaller than 0.5 mm, Izhar et al.[24] selected fractions below 0.2 mm, and Zhao et al.[25] used particles smaller than 0.165 mm. The literature offers limited insight into the energy requirements and rationale for grinding biochar for use as a soil amendment, underscoring a critical knowledge gap. In addition to sieving, some of the biochar produced underwent activation processes. Chemical activation was commonly conducted using KOH[30,33,35,39,47] and occasionally $ZnCl_2$.[33] For physical activation, agents such as CO_2,[35,39,42] steam,[32,35,42] or O_2/N_2[32] were employed. Notably, in the study by Xu et al.[42] activation was carried out during pyrolysis rather than after introducing the activation agent into the reaction zone while pyrolysis was ongoing. Juntarachat and Onthong[29] introduced an innovative method to prepare biochar adsorbents by extruding the biochar into spherical shapes using starch as a binder.

In conclusion, the literature review suggests that feedstock is typically dried between 45°C and 110°C before pyrolysis. There is no uniform agreement on particle size for pyrolysis, with studies using finely milled materials (0.106 to 2 mm), coarsely crushed materials (30 to 500 mm), and raw and pelletized forms. In cases of highly contaminated feedstock, washing was sometimes performed. Various equipment types were employed to produce biochar, the most common being lidded containers heated in a muffle furnace and tubular reactors. Other methods included the use of fluidized bed reactors, screw reactors, microwave reactors, traditional kilns, and cyclonic bed reactors. Biochar was generally produced by slow pyrolysis, with heating rates of 5 to 22°C/min, at temperatures of 400, 500 or 600°C and residence times of a few hours or less. Most studies on pyrolysis have focused on processes conducted at atmospheric pressure in an inert atmosphere, typically nitrogen or argon, or under limited oxygen conditions. The resulting biochar was utilized to remove sulfur compounds, either in their raw state or after being sieved into fractions with particle sizes ranging from 0.165 mm to 2 mm. They were frequently subjected to chemical activation, typically with KOH or physical activation using CO_2, steam, or O_2/N_2.

EXPLORING THE PROPERTIES OF PURE VS. SULFUR-ENHANCED BIOCHAR

Biochar characterization is based on understanding its structure, identifying surface functional groups, and analyzing its elemental composition.[3] This section highlights key

Table 2. pH values of selected biochars produced from waste biomass.

Biochar raw material	Pyrolysis temperature	pH	Ash (%)	Ref.
Oil palm fiber (OPF)	450°C	6.78	10.0	[38]
Palm oil sludge (POS)	442°C	7.01	53.1	[41]
Black spruce (BS)	454°C	7.10	n.a.	[35]
White birch	454°C	5.90	n.a.	[35]
Palm oil mill sludge (POMS)	400°C	6.82	44.8	[44]

parameters and techniques used for biochar characterization and their application in studies on sulfur compound adsorption.

pH

pH is an essential parameter in biochar characterization, as it affects its quality and possible applications.[9] The pH of biochar can influence several properties, including acidity/alkalinity, nutrient availability, suitability for soil amendment, and stability.[55] Table 2 shows examples of biochar pH values and ash content obtained from waste biomass. The pH difference between biochars may result from variations in the contents of alkali, alkaline earth metals, and carbonates.[56] The biochars presented in Table 2 were produced at a similar temperature during the pyrolysis process. It can be seen that the higher the ash content in biochar, the higher the pH of the biochar. In the case of the ash content, it increases as the pyrolysis temperature rises. This is most likely owing to the mineral component, which converts into ashes with higher heating treatment.[41]

According to the literature, a pH value lower than 7 indicates that the acidic surface of biochar will be ineffective in removing sulfur from the gas phase.[38] However, a biochar with a pH value higher than 7 tends to have more alkaline properties and is conducive to sulfur adsorption, indicating an alkaline surface since SO_2 is an acidic gas. Hence, when SO_2 comes into contact with the biochar alkaline surface, it is adsorbed easily. On the contrary, biochar with a low pH may exhibit different adsorption behavior due to its acidic nature, which can influence the type and amount of sulfur it sorbs.[57] Generally, the lower pH of biochar can promote the adsorption of more acidic sulfur species, particularly SO_4^{2-} and SO_3^{2-} ions, as well as elemental sulfur under specific conditions.[25] Xu et al.[56] showed that the biochars tested in their study (dairy manure, sewage sludge, and rice husk biochar) had a pH value above 8.9. They also found that the presence of H_2O may promote the development of an alkaline water membrane on the surface of the biochar, which facilitates the removal of acidic SO_2. After SO_2 sorption, biochars showed a significant decrease in pH.

Elemental Composition

The elemental composition (C, H, N, S) of biochar depends to a large extent on the raw material from which it was produced. For example, Xu et al.[56] compared the elemental composition of their produced biochars. Rice husk biochar had the highest C content, which is typical for biochars derived from plant residues. In contrast, sewage sludge and dairy manure biochar had a much higher content of N, S and macro- (Ca, Mg, P) and microelements (Fe, Mn). The elemental composition of biochar changes with the temperature of the pyrolysis process. A few examples are presented in Table 3. The pyrolysis heating temperature had a significant impact on the carbon, hydrogen, nitrogen, and sulfur content. For example, the carbon content of biochar from oil palm fiber ranges from 44.8 to 76.0% at temperatures of 200 to 600°C.[38] The C content of palm oil sludge biochar ranges from 30.1 to 31.4% at temperatures of 300 to 700°C, respectively.[41] In general, the carbon content of biochar increases with increasing temperature. The increase in carbon content corresponds to a decrease in hydrogen at higher pyrolysis temperatures, which is caused by the cleavage of weak bonds within the feedstock structure.[60] However, in the case of biochar produced from the microalga *Chlorella* sp., the carbon content displayed irregular behavior, deviating from the expected trend typically observed at increasing pyrolysis temperatures. This could be a result of variations in feedstock heterogeneity.[58] At the same time, the hydrogen content systematically decreased, dropping from approximately 4.19% at 400°C to 1.32% at 700°C and further declining to less than 1% at 800–900°C. For nitrogen, an increase in its content was observed in the biochar produced at 400°C (9.72%), likely due to the incorporation of this element into the biochar structure. On the other hand, sulfur was not present in all the biochar produced from microalgae.[58] The nitrogen content in biochar generally decreases with increasing pyrolysis temperature due to the thermal decomposition of nitrogen-containing compounds, such as amines and amides. This process results in the release of nitrogen gas and other nitrogenous gases, such as NH_3 and HCN, thereby reducing the overall nitrogen content remaining in the biochar.[61] Furthermore, as the pyrolysis temperature increases, the S content augments rather than decreases, possibly due to the limited amount of sulfur in volatile compounds. Then, even at higher temperatures, there may simply be fewer sulfur compounds available to volatilize. This could lead to more sulfur being retained in the solid residue.[62]

The sulfur content can increase significantly in biochar if it is used as a biosorbent to remove sulfur (examples given in Table 1) in various forms, such as SO_2 from industrial activity

Table 3. Elemental composition (%) of biochars produced from waste biomass.

Biochar raw material	Pyrolysis temperature	C	H	N	S	Ref.
Oil palm fiber	200°C	44.8	4.95	0.20	0.00	[38]
	450°C	73.9	3.76	0.71	0.25	
	600°C	76.0	1.77	0.36	0.00	
Palm oil sludge	300°C	30.1	2.60	3.88	0.49	[41]
	442°C	31.9	2.01	3.76	0.52	
	700°C	31.4	0.93	1.61	0.73	
Microalga	400°C	58.8	4.19	9.72	<0.01	[58]
Chlorella sp.	500°C	61.6	3.76	8.68	<0.01	
	600°C	56.8	1.53	6.73	<0.01	
	700°C	55.7	1.32	7.72	<0.01	
	800°C	56.7	0.88	6.72	<0.01	
	900°C	53.2	0.85	4.72	<0.01	
Willow chips	440°C	51.3	n.a.	1.09	0.11	[59]
	475°C	54.7	n.a.	1.07	0.13	
	530°C	43.8	n.a.	0.82	0.06	

(e.g., power plants), from the combustion of fossil fuel or waste incineration, H_2S from municipal solid waste, biogas, gas streams, livestock environment, or SO_4^{2-} ions from aqueous solutions, for example sodium sulfate solution. In summary, the elemental composition of biochar depends mainly on the type of biomass used and the pyrolysis conditions during its production.

Thermogravimetric Analysis

TGA is a thermal analysis technique used to study how the physical and chemical properties of a material change as it is heated.[9,63] The thermal stability of biochar is a crucial consideration when evaluating its potential use as a soil amendment or for carbon sequestration.[64] TGA also enables the quantification of sulfur retained within the biochar, providing insights into its thermal stability. During controlled heating, volatile components, including various sulfur species, are released, resulting in measurable mass loss. By analyzing these changes, it is possible to determine both the amount of sulfur effectively adsorbed and the temperature ranges at which specific sulfur compounds and biochar constituents decompose. This information is essential for understanding the mechanisms of sulfur adsorption, transformation, and retention, as well as for assessing the suitability of biochar for environmental and agricultural applications where thermal stability and nutrient retention are critical.[65] Significant is the determination of the temperature at which biochar begins to decompose, as it defines the maximum thermal load the material can withstand before degradation. If this decomposition temperature is too low, the biochar may lack sufficient thermal stability for applications that involve elevated temperatures.[66]

Jayaraman et al.[67] used TGA-MS, combined with kinetic analysis, to assess the pyrolysis and gasification of sugarcane bagasse at three heating rates: 10, 50, and 100°C/min. At the slow heating rate (10°C/min), gases (CO_2, CO, CH_4) were released gradually, indicating uniform decomposition of the material. Faster heating (100°C/min) resulted in rapid and intense gas evolution, reflecting accelerated decomposition of the organic components. The char yield after pyrolysis was inversely proportional to the heating rate: slow heating increased the yield due to more complete decomposition of volatile components, whereas fast heating resulted in lower char yield due to rapid volatilization.

Fourier Transform Infrared Spectroscopy

FTIR is an analytical tool used to examine the functional groups on the surface of biochar. It can also be utilized to examine how the temperature and heating duration affect the surface functional groups of biochar.[9] The FTIR method can also confirm the successful activation of biochar, enabling the incorporation of additional oxygen-containing groups that improve the surface functionality.[68] Table 4 presents examples of functional groups found in biochars produced at different temperatures from palm oil sludge (POSAB) and sugarcane bagasse, which were used for the removal of SO_x. The wavenumbers for the determined functional groups in POSAB biochar produced at 300 and 442°C were almost identical. Only slight variations in the wavenumbers and intensities were observed, indicating minimal variations in the surface chemical composition of biochar produced at these temperatures. Peaks were observed for POSAB produced at 300, 442 and 700°C, respectively, at 1590 cm^{-1}, 1600 cm^{-1} and 1700 cm^{-1}. The aromatic system of double bonds between carbon atoms was observed, as evidenced by peaks between 1590 and 1700 cm^{-1},[69–72] as well as aromatic double bonds between carbon and oxygen atoms. Additional peaks for POSAB biochar produced at 300°C and 442°C were also seen at 1390 cm^{-1} and 1410 cm^{-1}, while for biochar produced at 700°C, 1370 cm^{-1} and 1268 cm^{-1} were observed.

Iberahim et al. [41] presented FTIR spectra of palm oil-activated sludge biochar before and after sulfur adsorption. The spectra show that additional peaks have emerged on POSAB produced at 442°C. After sulfur adsorption, a significant peak at 1739 cm^{-1} was seen, indicating C=O stretching of carbonyl, aldehyde, ketone and ester.[71,72] Additionally, significant peaks were found at 1365 cm^{-1} and 1261 cm^{-1}. Peaks in this range typically represent sulfur-containing functional groups that may have changed during adsorption.[73] Furthermore, a significant peak at 1365 cm^{-1} corresponds to the adsorbed form of SO_2.[74] The last peak observed at 1019 cm^{-1}, after adsorption, shows no difference compared to a new adsorbent, indicating that the functional group associated with this peak has a minimal influence on the adsorption activity. Therefore, it is concluded that the functional groups present on the surface of the adsorbent play an essential role in the SO_2 adsorption efficiency.[75–77] Iberahim et al.[44] indicated

Table 4. Major functional groups of palm oil-activated sludge biochar and sugarcane bagasse biochar determined by FTIR spectra.

Biochar raw material	Pyrolysis temperature	Functional groups	Ref.
Palm oil-activated sludge	300°C	C=C / C=O (1590 cm^{-1}), , C-O / O-H (1390 cm^{-1}), C-O (1008 cm^{-1})	[41]
	442°C	C=C / C=O (1600 cm^{-1}), , C-O / O-H (1410 cm^{-1}), C-O (1018 cm^{-1})	[41]
	700°C	C=C / C=O (1700 cm^{-1}), C-O / O-H (1268 cm^{-1}, 1370 cm^{-1})	[41]
Sugarcane bagasse	700°C	OH (1674 cm^{-1}), C=O (3495 cm^{-1}), C-H (2974 cm^{-1}), C-H_2 (2853 cm^{-1}), C-O (1068 cm^{-1}), N-H (3487 cm^{-1}) COOH (2900–3500 cm^{-1})	[26]

that palm oil mill sludge biochar adsorbs SO_2 mainly through its functional groups. It was found that biochar obtained at 400°C is characterized by a better structure of functional groups, which significantly improves the SO_2 adsorption capacity compared to biochars obtained at higher temperatures (500, 600, 700 and 800°C), which are characterized by a decreasing number of functional groups – high temperatures could destroy these groups.[44] Generally, the active surface of the biochar should be basic to enhance the adsorption of sulfur dioxide, because it is an acid gas. The basic sites on the surface of biochar are associated with both surface oxygen and nitrogen-containing groups.[41]

Brunauer-Emmett-Teller Analysis

BET analysis can be used to determine the surface area of biochar, a crucial measurement for understanding its adsorption capability, reactivity and utilization.[9] A higher BET surface area generally means more surface is available for interactions with other substances, such as gases or pollutants, making it useful in various environmental and agricultural applications. According to Bonelli et al.[78] increasing the pyrolysis temperature results in changes to the surface area and porosity of the biochar. This means that as the pyrolysis temperature rises, the surface area of biochar typically increases. Similarly, the formation of micropores and mesopores increases with increasing temperature, resulting in a biochar structure with enhanced porosity. This is most likely due to the decomposition of organic matter at higher temperatures, which exposes more carbon structures and generates additional surface area.[79]

Table 5 shows, for example, the BET surface area, Langmuir surface, and micropore volume of oil palm fiber and palm oil mill sludge (POMS) biochar produced at different pyrolysis temperatures (400, 500, 700 and 800°C). The results show that the surface area of the POMS biochar obtained at 800°C was 193 m^2/g, which appears to be the largest among the other POMS biochars. This indicates that a pyrolysis temperature of 800°C is more suitable for the adsorption of SO_2 by biochar produced at this temperature.[44] This is because an increase in the surface area of biochar provides a greater number of adsorption sites and spaces for SO_2.[38] Additionally, the large BET surface area represents the entire surface area inside the pores that is available to gas molecules, including both internal and external surfaces. Because adsorption can occur inside pores and on their external surfaces, particularly in the case of micropores, this results in an increase in the volume of the micropores and a larger Langmuir surface area. As seen in the case of POMS at an 800°C pyrolysis temperature, it exhibits a large BET surface area, resulting in a 257 m^2/g Langmuir surface area and micropore volume (0.065 cm^3/g). This means that 800°C POMS have a more available surface area for SO_2 adsorption than other biochars, particularly oil palm fiber, which had the least space for sulfur to be adsorbed.

Iberahim et al. found that biochar produced from oil palm fiber at temperatures of 600, 753 and 800°C and activated using CO_2 (OPFAB) showed the highest 271 m^2/g BET surface area when produced at 753°C.[28] Activation of biochar with CO_2 promotes the development of a mesoporous structure, which enhances its surface area. This biochar showed the highest SO_2 adsorption capacity. Additionally, it was well correlated with the high carbon and fixed carbon content in OPFAB 753°C.[28] The authors speculated that this may be one of the primary reasons why this OPFAB is the most effective adsorbent for SO_2 adsorption. They also indicated that the pore size of OPFAB at 753°C was smaller than that of oil palm fiber biochar and other activated biochars at different temperatures, which may be one of the main factors explaining the optimal adsorption of SO_2 gas at 753°C.[38] Opposite results were obtained by Xu et al.[56] who used biochars derived from dairy manure (DM-biochar), sewage sludge (SS-biochar), and rice husk (RH-biochar) for SO_2 removal. The selected physicochemical properties, such as biochar specific surface area and pore volume, followed the order: RH > SS >DM-biochar. But, the contrary trend was observed for the SO_2 sorption capacity by biochar: DM > SS >RH-biochar. The authors suggested that this discrepancy may indicate that SO_2 sorption by biochar was not controlled by its surface area but rather by inorganic components. The SO_2 sorption trend appears to be consistent with the mineral content in the biochars studied. Minerals in biochar can react with adsorbed SO_2 to form various sulfate minerals, which enhances SO_2 removal by biochar. This means that the specific surface area of biochar is not the only factor that describes the SO_2 adsorption capacity.

Scanning Electron Microscope – Energy Dispersive X-Ray Spectroscopy

SEM is used to study the surface morphology of raw materials. SEM images may also indicate an increase in the biochar surface area resulting from a higher pyrolysis temperature, which could favor SO_2 adsorption.[44] These images can also display the microporous and mesoporous distributions, as well as the pore structure, present in the biochar.[9,44] They can also be used to predict the surface shape before and after the adsorption process.[80] Iberahim et al.[44] using SEM images, demonstrated that among biochars produced from POMS at the temperature range of 300–800°C, pore structures of larger

Table 5. Bet analysis result of biochars produced from oil palm fiber and palm oil mill sludge.

Biochar raw material	Pyrolysis temperature	BET surface area (m^2/g)	Langmuir surface (cm^3/g)	Micropore volume (cm^3/g)	Ref
Oil palm fiber	450°C	1.31	3.12	0.0267	[38]
Palm oil mill sludge	400°C	47.7	65.3	0.0066	[44]
	500°C	35.3	49.2	0.0012	
	700°C	174	232	0.0513	
	800°C	193	257	0.0653	

sizes and shapes developed for biochar produced at 400°C, and the highest SO_2 adsorption capacity was characterized by it. Such biochar may have a larger surface area and can provide more adsorption sites. At a higher temperature of 800°C, the surface of the biochar had more cracks and larger holes.[44] Many authors have employed the SEM technique to visualize the surface area of biochar produced from waste biomass used for the adsorption of sulfur compounds. Examples include biochar from rice hull feedstock, banana peel, and sawdust[24]; biochar produced from corncobs, cassava rhizomes and cassava stems,[81] as well as palm oil sludge biochar.[41]

The elemental composition of the biochar surface before and after SO_2 sorption can be investigated using energy-dispersive X-ray spectroscopy (EDS) in conjunction with SEM.[9,80] However, this technique determines the elemental composition of the biochar surface. To determine the elemental content of the entire sample, inductively coupled plasma optical emission spectrometry is required, which is typically preceded by sample digestion, often performed in a microwave oven.

MECHANISM OF SULFUR REMOVAL BY BIOCHAR – INSIGHTS AND PROCESSES

To effectively carry out the adsorptive desulfurization of gases using porous carbon materials, including biochar, it is essential to understand the adsorption process and the behavior of adsorbate molecules within the adsorbent pores. In the case of SO_2, the literature regarding the adsorption mechanism of this gas on the surface of biochar is limited. Therefore, this section is based mainly on studies of activated carbon and coke. For H_2S, the literature is significantly more available. Although many of these works focus solely on laboratory-scale studies, they still represent an essential step toward understanding the adsorption process of this gas. Many authors indicate that the binding process of sulfur compounds has a dual nature, depending on the composition of the gas mixture and the nature of the interacting forces. Studies by Brunauer and Emmet [82] and Zhang et al. [60] demonstrated that in a dry gas environment and/or in the presence of molecular oxygen, the adsorption of SO_2 occurs due to weak van der Waals forces, typical of physisorption. The rate of this process is primarily limited by the diffusion of the adsorbate to the solid surface and its energetic effect is small, ranging from a few to several tens of kilojoules per mole. In contrast to these findings, Kisiela-Czajka [83] states that SO_2 accumulation can occur through both physical and chemical adsorption, even in mixtures devoid of H_2O and O_2. The author emphasizes that the oxidation of SO_2 to SO_3 is due solely to oxygen from the gas phase, not from oxygen weakly bound to the surface of the carbon substance, as is confirmed by Qu et al.[84] Lizzio and DeBarr[85] and Jing et al.[86]

Similar to SO_2, H_2S adsorption can be dual, involving both physical and chemical processes. It has been observed that the amount of adsorbed H_2S increases with increasing temperature.[87] Furthermore, the study by Han et al.[46] indicated that lower temperatures favor physical adsorption, while an increase in temperature promotes the permanent binding of the adsorbate. The mechanism of gas pollutant adsorption on carbon materials has been extensively described,[88] and the removal of SO_2 from actual flue gases has been investigated.[89–92] However, many authors who focus on maximizing the efficiency of the SO_2 removal process simplify the representation of its adsorption and conversion to sulfuric acid (H_2SO_4) according to the reaction:

$$SO_2 + {}^1/_2O_2 + H_2O(g) \rightarrow H_2SO_4 \quad (1)$$

The complexity of carbonaceous substances complicates the interpretation of research results, as highlighted in the works of Lizzio and DeBarr,[85] Annurov,[93] and Lisovskii et al.[94] Despite similar experimental conditions (20–150°C, 5–10% oxygen), the obtained results are contradictory (Figure 7). According to Lizzio and DeBarr[85] (see Figure 7a), the oxidation of SO_2 to sulfuric acid (S_{VI}) occurs through the reaction of the C-SO_2 complex with oxygen:

$$C - SO_2 + O_2 + C \rightarrow C - SO_3 + C - O \quad (2)$$

$$C - SO_3 + H_2O \rightarrow C - H_2SO_4 \quad (3)$$

On the other hand, Annurov[93] (see Figure 7b) points out that an oxygen content in flue gases below 10% is insufficient for the complete oxidation of SO_2 to SO_3. Based on his experimental results, he postulates that the physisorption of SO_2 is associated with the formation of a weak and unstable sulfurous acid (IV), which, upon reacting with molecular oxygen from the gas phase, forms sulfuric acid (VI):

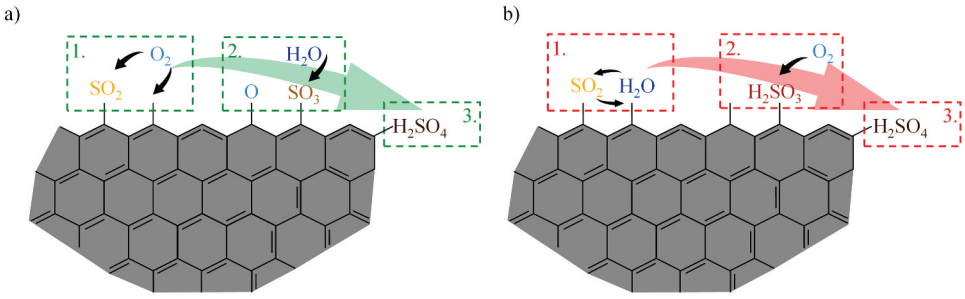

Figure 7. Mechanisms of SO_2 adsorption on carbon materials. Symbols: (a) according to Lizzio and DeBarr[85]; (b) according to Annurov.[93]

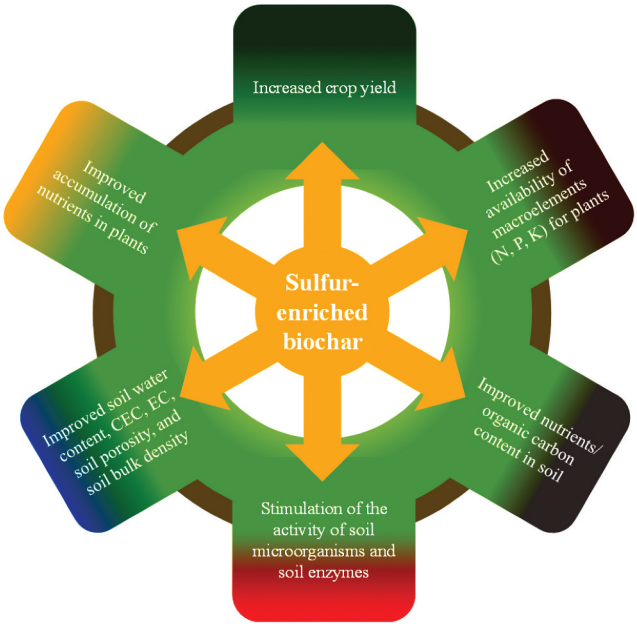

Figure 8. The positive effect of sulfur-enriched biochar on plant growth and soil properties.

$$C - SO_2 + C - H_2O \leftrightarrow C - H_2SO_3 \quad (4)$$

$$C - H_2SO_3 + O_2 \leftrightarrow C - H_2SO_4 \quad (5)$$

This hypothesis has not yet been definitively confirmed. This may be because H_2SO_3 is unstable, which significantly complicates its identification and characterization. Interestingly, an appropriate amount of water vapor can positively influence the efficiency of sulfur compound adsorption on the surfaces of carbon adsorbents. According to research results,[93] the most significant differences in the amount of adsorbed SO_2 occur at water vapor concentrations in the gas mixture of up to 8% v/v. In our study,[83] it was demonstrated that with an 11% share of $H_2O_{(g)}$, the total sulfur concentration in the solid phase showed a slight decrease compared to the total sulfur concentration corresponding to SO_2 adsorption under dry gas mixture conditions. It can be assumed that the sulfurous acid formed, due to the high chemical affinity of SO_2 for water, was oxidized to sulfuric acid (VI), whose presence, in turn, blocks the active sites capable of oxidizing SO_2.

Han et al.[46] demonstrated that the adsorption efficiency of H_2S decreases with increasing H_2O concentrations in the range of 5–10%. As noted by Yang et al.[95] an appropriate amount of moisture promotes the ionization of H_2S, leading to the formation of the HS^- ion. However, an excess of moisture can result in condensation, creating a water film on the surface of the adsorbent, which blocks pores and hinders the adsorption of H_2S. Considering that the SO_2 molecule has a bent shape with S=O bond lengths of approximately 0.143 nm and a bond angle of 119°, its average dimension can be estimated at around 0.3–0.4 nm, suggesting that ultramicropores play a crucial role in the adsorbent adsorption capacity. According to Raymundo-Pinero et al.[96] although the adsorption of SO_2 from a gas mixture devoid of oxygen and water vapor increases proportionally to the volume of the adsorbent micropores, in the case of a mixture containing O_2, it can reach a maximum in pores approximately 0.7 nm wide. Hence, due to the geometry of the SO_3 molecule and its greater spatial extent compared to SO_2, there are more favorable conditions for SO_2 oxidation in micropores larger than 0.4 nm, thereby increasing the adsorption potential of the material. Studies by Kisiela-Czajka[83] elaborated on the correlations described by Raymundo-Pinero et al.[96] Moreno-Castilla et al.[97] and Wang et al.[98] indicating that the effectiveness of the analyzed process is influenced not only by the spaces between the carbon material grains but also by the degree of development of its porous structure. An effective prediction of the utility of a given material in the context of desulfurization also requires considering the method of bed formation, including the free interstitial spaces.

Another issue is the adsorption in the presence of oxygen and water vapor, as described by Bansal and Goyal,[99] confirmed by Izquierdo and Rubio[90] and Kisiela-Czajka.[83] Optimal conditions for SO_2 adsorption are achieved with materials that have a moderately developed microporous structure, which limits the formation of stable carbon-sulfuric acid (VI) compounds, thereby preventing the desorption of these compounds and blocking active sites capable of oxidizing SO_2. Based on the adsorption studies described in Annurov,[93] conducted with various adsorbents, it was concluded that the presence of mineral substances limits the adsorption capacity of SO_2, which results from the deterioration of the adsorbent textural parameters. Research [83] indicates that the reaction of Al_2O_3 with ash leads to the irreversible formation of $Al_2(SO_4)_3$. The presence of this compound on the surface, along with desorbing sulfuric acid (VI), may block active sites capable of forming chemical bonds with adsorbate molecules.

For many years, research on the desulfurization of flue gases has also focused on the relationships between the adsorption capacities of carbonaceous adsorbents and their chemical structure.[35,75,90,96,100,101] A contradiction exists in the findings of various authors. According to Cen et al.[102] SO_2 adsorption increases with the content of strongly acidic oxygen-containing functional groups which serve as adsorption sites for the polar adsorbate, while analyses by Izquierdo and Rubio [90] and Atanes et al.[75] provide evidence that high surface basicity is also observed. We thoroughly analyzed these contradictions, indicating that, in the absence of oxidative adsorption of SO_2, acidic functional groups have a positive effect.[83] On the contrary, the process of SO_2 adsorption, associated with its oxidation to SO_3 and the formation of H_2SO_4, is correlated with the presence of weakly acidic (phenolic) and neutral (carbonyl) or basic carbon-oxygen functional groups. The correlation between the presence of oxygen-containing functional groups and the effectiveness of SO_2 adsorption is not supported by the studies described by Raymundo-Pinero et al. [96] and Wang et al.[98] They suggested that, contrary to popular belief, it is the nitrogen surface groups, rather than the carbon-oxygen functional groups, that have a positive influence on the amount of adsorbed SO_2. They demonstrated that pyridinic nitrogen enhances the catalytic activity of porous carbonaceous materials in SO_2 oxidation reactions.

Han et al.[46] highlighted that the efficiency of H_2S adsorption depends on the conditions under which the biochar is produced. In the case of algae-based biochar, a significantly higher H_2S adsorption efficiency was observed for samples produced at higher temperatures (800°C > 600°C > 400°C). It was suggested that higher calcination temperatures promote the formation of more basic surface groups (e.g., carboxylate groups COO^-), which positively influence H_2S adsorption. It was also demonstrated that increasing the calcination temperature supports the development of the micro- and mesoporous structure of the biochar, which is crucial for effective H_2S adsorption. These findings are consistent with the observations reported by Sahota et al.[45]

APPLICATION OF SULFUR-ENRICHED BIOCHAR IN AGRICULTURE

Biochar is known for numerous agricultural and environmental benefits, such as increasing crop yields and improving soil properties including structure, fertility, nutrient retention and availability, water-holding capacity, organic carbon content, biomass, and microbial and enzymatic activity, as well as reducing environmental impacts, carbon sequestration and greenhouse gas emission mitigation.[103] In addition, the use of nutrient-enriched biochar as a soil amendment may reduce the need for mineral fertilizers. In the long term, such biochar may be more beneficial for maintaining soil fertility due to its high organic matter content and the gradual release of micronutrients compared to conventional chemical fertilizers. Its positive effects on the content of micro- and macronutrients, soil organic matter, and biomass yield indicate that enriched biochar may also support the development of organic agriculture.[15,103,104]

A particular importance is attributed to sulfur-enriched biochars (see Figure 8). Sulfur is an essential macronutrient involved in key plant metabolic processes, as it is a component the cysteine and methionine amino acids. Cysteine plays an important role in the formation of enzyme active sites, sulfhydryl groups, and disulfide bridges in proteins.[105] In addition, sulfur exhibits biologically active properties, including bactericidal and insecticidal effects.[106] It has been shown that the presence of sulfur functional groups C–S, C=S, may influence the structure of soil microbial communities, increasing the abundance of copiotrophic groups such as *Proteobacteria*, *Bacteroidetes*, and *Actinobacteria*, which are associated with intensive organic matter decomposition and nutrient cycling, while reducing the abundance of oligotrophic groups such as *Acidobacteria* and *Gemmatimonadetes*, which are typical of nutrient-poor soils.[107]

The sulfur content in biochars is typically low, which results from its limited presence in the original feedstocks and from transformations occurring during thermal biomass conversion. At the same time, the surface of biochars is dominated by oxygen- and carbon-containing functional groups.[108,109] The mechanisms of sulfur speciation during pyrolysis remain complex; however, available studies indicate a significant influence of process conditions, particularly temperature, as demonstrated by Cheah et al.[110] X-ANES analyses show that with increasing pyrolysis temperature, the SO_4^{2-} and S^{2-} proportion decreases, while the organic sulfur proportion increases. In oak bark biochar, over the temperature range 500–850°C, a systematic decrease in the sulfate fraction (56% → 26% → ~0%) is observed, accompanied by a corresponding increase in the organosulfur fraction (44% → 62% → 100%), with a transient presence of sulfides at 600°C (12%). To increase the sulfur content in biochar, various strategies have been developed, including feedstock selection, optimization of pyrolysis conditions, and post-process modification. Among these, sulfur doping is the most commonly applied approach, implemented either during pyrolysis or via post-impregnation using S-containing compounds such as $Na_2S_2O_3$, H_2SO_4, and Na_2S.[111,112] The introduced S atoms are predominantly located on the biochar surface, where they can interact with reactive sites associated with unpaired electrons at the edges of aromatic carbon structures.

In the case of biochars exposed to SO_2 under oxygen-limited conditions, their chemisorption on the material surface and the formation of S-containing functional groups are observed. Our own study on biochar derived from mandarin peel pomace[108] showed an intensification of FTIR bands in the 3600–650 cm^{-1} range linked to the formation of surface sulfur groups ($–SO_3H$, $–SO^{3–}$). Changes in the 3600–3000 cm^{-1} and 1750–1450 cm^{-1} regions indicate the involvement of –OH and C=O groups in surface reactions, leading to the formation of oxidized sulfur species (S(IV)/S(VI)), while an increase in the intensity of bands in the 900–650 cm^{-1} range may indicate sulfonation of the edges of aromatic structures. Despite the growing number of studies, the mechanism by which sulfur is released from biochar into soil remains poorly understood. However, available data indicate that the dominant form of sulfur in soil after biochar application is the SO_4^{2-} ion, which represents the most readily available form for plants. Sulfate release occurs gradually through desorption of surface-bound forms and microbial mineralization of organic sulfur. Churka Blum et al. [113] showed that this process begins within the first days of incubation, with inorganic sulfates being the main sulfur species in the soil solution. Under aerobic conditions and in the presence of moisture, further oxidation of reduced sulfur forms to SO_4^{2-} is also possible.

The Effect of Sulfur-Enriched Biochar on Plant Growth Parameters and Soil Properties

Zhang et al. [13] conducted a greenhouse study examining 36.5% S-enriched biochar, produced from anaerobically digested solid dairy manure, as a potential soil amendment for corn (*Zea mays*) and soybeans (*Glycine max*). This biochar was produced by passing biogas emitted from a landfill through a column packed with biochar. The growth of corn in the group with sulfur-enriched biochar was significantly greater than the growth obtained after the application of mineral fertilizer with magnesium sulfate at the same sulfur dose. Steam activation of biochar increased the number of micropores and mesopores, which enhanced water adsorption and SO_2 retention, a by-product of H_2S oxidation. It accelerated the oxidation of H_2S to S, SO_2 and/or SO_4^{2-}. This study confirmed that the adsorbed and oxidized H_2S contained in biochar was available to plants and supported their growth by providing them with a source of sulfur for uptake. Taheri

et al.[15] produced a S-modified biochar by mixing sunflower biochar with an inorganic sulfur solution. The 1.4% S biochar produced was tested in the cultivation of millet (*Proso*) in saline and calcareous soil under field conditions at a dose of 15 t/ha. This study demonstrated that the application of S-enriched biochar increased the millet yield by 115% by enhancing soil water content by 35% and nutrient content, particularly phosphorus, compared to the control. It also increased the soil-dissolved organic carbon by 33%, available N by 48%, and available P by 96% compared to the control.

Sulfur-enriched biochar is a proposed solution for increasing P availability in plants[114] by lowering the soil pH.[15] This approach was employed by Zimmer et al.[114] using P-rich bone char, which could serve as an alternative phosphorus fertilizer in sustainable agriculture, but is characterized by low P solubility. Enrichment of bone char with sulfur decreased its pH from 8.6 to 5.0. The atom S % in the S-enriched biochar ranged from 3 to 4% (SEM-EDX). S oxidation by microorganisms and the subsequent acidification of the soil increased the solubility of phosphorus, making it more available to plants. A pot experiment with annual rye grass (*Lolium multiflorum* L.) treated with bone char, S-enriched bone coal, and the mineral fertilizer – triple superphosphate showed that the grass yield and apparent nutrient recovery efficiency in the group treated with enriched biochar were similar to superphosphate and that it has potential as a P and S fertilizer. The increase in the availability of nitrogen to plants as a result of applying S-modified biochar to the soil may be due to the increased activity of the urease enzyme, the provision of appropriate conditions for the development of soil microorganisms and the enhancement in the concentration of ammonium and nitrate ions in the soil, which are readily available to plants.[15] Taheri et al. [15] found that the supplementation of the soil with S-enriched sunflower biochar stimulated the activity of soil microorganisms and enzymes, especially urease, catalase, dehydrogenase, and alkaline phosphatase. Enzymatic activity of the soil can be increased when the organic compounds are easily decomposed.

In biochar, the higher the O/C and H/C molar ratio, the lower the carbon stability and aromatic carbon content, and the easier decomposition of compounds.[115] Taheri et al.[15] reported that these ratios in the S-enriched biochar from residue of sunflower stalks were higher than in the pristine biochar, which may suggest that carbon and nutrients will be released into the soil and absorbed by plants more quickly. Finally, in the group treated with biochar, the accumulation of plant nutrients, such as N, P, and K, as well as the relative leaf water content, increased compared to the control group. El-Sharkawy et al.[14] obtained S-enriched biochar by mixing it with sulfuric acid. Rice straw and cotton stalks were used as raw material for pyrolysis. The effect of this biochar on the growth of maize (*Zea mays*) and wheat (*Triticum aestivum*) in saline soils was examined in a field experiment. Similar to the publication by Taheri et al.[15] the addition of modified biochar to the soil increased the availability of N, P and K compared to pristine biochar. Also, it enhanced the accumulation of these elements in cultivated plants. Grain/straw yield for maize increased by 34.2% and 29.8% and for wheat by 25.1% and 15.0% when grown in soil amended with S-modified biochar produced from cotton stalks compared to the control.

The addition of S-modified biochar to a soil in which maize and wheat were grown under abiotic stress conditions (saline soil) resulted in increased accumulation of proline and the activity of antioxidant enzymes such as superoxide dismutase, catalase and peroxidase. Zhang et al.[13] tested biochar obtained from anaerobically digested solid dairy manure, additionally activated by steam, for the adsorption of H_2 S. S-enriched biochar, containing 36.5% S, was used as a soil amendment in the cultivation of corn and soybean (*Glycine max* (L.) Merr.) in a greenhouse study. The authors confirmed that the sulfur contained in the enriched biochar was available to plants and supported plant growth by providing a source of sulfur for plant uptake. S-enriched biochar also increased the uptake of other macroelements – N, P, K, Ca and Mg and micronutrients – Zn, Mn and B by corn, as well as yield, for corn ranging from 31% to 49% and for soybeans from 4% to 14%. El-Sharkawy et al.[14] also demonstrated that the use of S-enriched biochar from rice straw and cotton stalks enhanced the chemical and physical properties of the soil, including cation exchange capacity (CEC), soil organic carbon, soil bulk density, electrical conductivity and soil porosity. Enriching biochar with sulfur increases the number of hydroxyl and carboxyl functional groups on its surface, which increases the CEC of the biochar. Taheri et al. [15] confirmed that the presence of sulfate ions in S-modified biochar increased the CEC compared to pristine biochar.

The Effect of Sulfur-Enriched Biochar on Plant Resistance to Abiotic and Biotic Stress

Nowadays, crops are exposed to abiotic stress caused by drought, high salinity, waterlogging, temperature stress: heat stress, freezing, and chilling, and high concentrations of heavy metals in soil. These stress factors cause changes in the morphological, biochemical and physiological processes of plants, leading to reduced germination rates of seeds, plant growth, photosynthesis, respiration, disturbances in the activity of enzymes and hormones, increased oxidative stress, and ultimately to reduced crop yield. One of the promising and environmentally friendly approaches that can mitigate the effects of abiotic stresses on crops is the use of biochar.[116] Enriching biochar with sulfur may have additional benefits – S-containing compounds are known to be essential for plant protection against stress caused, for example, by heavy metals.[105,116] Biochar, due to its excellent sorption properties, has the ability to immobilize pollutants in the soil, thereby limiting their availability and toxic effects on plants.[104,117] Additionally, the sorption capacity of biochar can be significantly increased by enhancing its surface with functional groups. Improvement of surface functionality can be achieved by treating biochar with sulfur compounds (H_2SO_4, Na_2S, and $Na_2S_2O_3$), which allows the introduction of sulfur-based functional groups (C=S, C–S, S–S, S^{2-}, S–H, $-SO_3^{2-}$, $-SO_4^{2-}$) onto the biochar surface, improving metal ions adsorption.[68]

Pathak et al. [105] showed in pot experiments that S-modified (with sodium sulfide or thiourea) tea-waste

biochar improved rice growth in arsenic-contaminated soil and reduced arsenic accumulation in plants. By applying biochar to contaminated soil, heavy metals become less mobile being bound by biochar, which means that their bioavailability in the soil for plants is significantly reduced. Moreover, biochar remains stable in the soil for an extended period, ensuring a more lasting remediation effect. S-modified biochar improved plant morphology (shoot and root length and fresh and dry weight), content of pigments (chlorophyll, carotenoids), reduced malondialdehyde content, which is an indicator of membrane damage, decreased superoxide dismutase, glutathione peroxidase, and catalase activity compared to plants grown in soil contaminated with arsenic without the addition of biochar.

Another heavy metal that can negatively affect plant yield is mercury. Zhao et al. [118] tested a sulfur-modified biochar, produced from rice husk, as a soil amendment to stabilize mercury in polluted agricultural soil. Modification of biochar with sulfur in the context of mercury immobilization is significant because there is a strong binding affinity between S and Hg, which forms the highly stable compound HgS (cinnabar). Moreover, the sorption capacity of S-modified biochar produced from rice husk toward mercury ions was 73% higher than that of non-modified rice husk biochar.[119] Zhao et al.[118] examined the temporal change in Hg fractions by simulated aging in 5% S-rice husk biochar-treated soil. Highly stable species HgS and organo-complexed Hg were dominant fractions, whereas water-soluble, strongly complexed, and exchangeable Hg fractions were much smaller. Hu et al.[120] also used S-modified biochar, produced from oilseed rape straw, in pot experiments to immobilize Hg in paddy soil, during rice cultivation. The addition of S-enriched biochar significantly accelerated the microbial methylation of Hg in the rhizosphere soil, which may be due to the increased content of Cl^- and SO_4^{2-} in the rhizosphere soil after biochar application.

It is known that biochar not only stimulates beneficial soil microflora in the rhizosphere, but also affects plant resistance to disease-causing pathogens.[121] Peng et al.[106] showed that the S-enriched biochar, obtained by combining biochar produced from pepper straw with sulfur at low temperatures, presented five times greater bactericidal efficacy against foodborne pathogen – *Escherichia coli* and the notorious plant pathogen – *Ralstonia solanacearum* compared to sulfur alone. The minimum inhibitory concentration of the enriched biochar toward both bacteria was 0.6 mg/ml. Tested biochar accelerated sulfur redox reactions, generating free radicals, such as •OH, $SO_4^{\bullet-}$, and $O_2^{\bullet-}$ that have efficient bactericidal action. Additionally, the high mesoporous structure, polarity, catalytic activity of surface functional groups, and dispersibility of the S-enriched biochar increase the contact surface with bacteria, which significantly improved the effectiveness of the antibacterial action. These results suggest that S-enriched biochars can be considered an environmentally friendly and cost-effective choice for mitigating abiotic stress, positively affecting plant productivity by providing not only sulfur but also other micro- and macroelements crucial for plant growth.

Limitations and Concerns About Using Biochar as a Soil Amendment

Most studies involving the use of biochar as a soil amendment are conducted under controlled conditions (pot tests in laboratory/greenhouse settings), which may differ from field conditions, where factors such as weather, soil microorganisms, and soil heterogeneity must be taken into account. Therefore, field studies are necessary to confirm the effectiveness of biochar in diverse environmental conditions. Furthermore, most studies focus on the short-term effects of biochar on plant growth and soil properties. Longer-term studies are necessary to analyze the impact of biochar on soil physicochemical properties, carbon sequestration, and its effects on soil microorganisms. When applying biochar as a soil amendment, special attention should be paid to the raw material from which it is made, as it may contain heavy metals that can be released into the soil, posing a threat to living organisms and negatively impacting environmental quality. In addition to heavy metals, biochar may also contain other pollutants such as polycyclic aromatic hydrocarbons, polychlorinated dibenzodioxins, and dibenzofurans, which could be produced during pyrolysis.[103] Biochars, mainly produced at high pyrolytic temperatures (≥600°C), are known to immobilize pollutants in the soil; however, they can also bind valuable micro- and macronutrients, thereby limiting their availability to plants and resulting in yield reductions. Before applying biochars to the soil, they should be carefully checked whether all requirements specified in applicable laws are met.

Biochars are recognized as a Component Material Category 14: Pyrolysis and gasification materials (Commission Delegated Regulation (EU) 2021/2088 of 7 July 2021) for EU fertilizing products (Regulation (EU) 2019/1009 of the European Parliament and of the Council of 5 June 2019 laying down rules on the making available on the market of EU fertilizing products). According to this Regulation, "the pyrolysis and gasification materials shall have a molar ratio of hydrogen to organic carbon (H/C_{org}) of less than 0.7, with testing to be performed in the dry and ash-free fraction for materials that have an organic carbon content of less than 50%." They shall have no more than: (a) 6 mg/kg dry matter of PAH_{16}, (b) 20 ng WHO toxicity equivalents of polychlorinated dibenzo-p-dioxins and dibenzofurans (PCDD/F)/kg dry matter, (c) 0,8 mg/kg dry matter of ndl-PCB (non-dioxin-like polychlorinated biphenyls). Furthermore, if biochar is to be placed on the market as an organic soil improver, it should meet the requirements for this Product Function Category (PFC) under Regulation (EU) 2019/1009. PFC descriptions include general thresholds for heavy metals, nutrients, carbon, pathogens, etc. Contaminants in an organic soil improver must not exceed the following limit values: (a) cadmium (Cd): 2 mg/kg d.m., (b) hexavalent chromium (Cr VI): 2 mg/kg d.m., (c) mercury (Hg): 1 mg/kg d.m., (d) nickel (Ni): 50 mg/kg d.m., (e) lead (Pb): 120 mg/kg d.m., and (f) inorganic arsenic (As): 40 mg/kg dry matter. The copper (Cu) content in an organic soil improver must not exceed 300 mg/kg d.m., and the zinc (Zn) content in an organic soil improver must not exceed 800 mg/kg d.m.

CHALLENGES AND FUTURE DIRECTIONS

The circular economy is a production and consumption model that focuses on maximizing the life cycle of products and minimizing waste. A key tenet is the reuse of raw materials and waste through recycling. This review aligns with a closed-loop economy by examining the dual use of bio-waste, first as a raw material for activated carbons and then as a post-consumption soil improver/organic fertilizer. The potential for the adsorption of sulfur compounds by activated carbons obtained from a variety of bio-wastes, such as agricultural waste, wood residues, food waste, biological sludge, municipal waste, and algae, was assessed. Particular attention has been given to the potential use of S-enriched adsorbents as soil improvers/organic fertilizers, thus closing the elemental cycle.

Although waste biomass-based activated carbons are often considered environmentally favorable, a comparative life cycle assessment [122] shows that their environmental performance strongly depends on the activation method, energy demand, chemical inputs, and production scale. Coconut-derived activated carbon exhibits relatively low climate impact, at approximately 5 kg CO_2-eq per kg. In contrast, sawdust- and wheat-based materials show higher impacts of approximately 8 and 11 kg CO_2-eq per kg, respectively, exceeding values reported for coal-derived activated carbon. For coconut-based activated carbon, over 90% of greenhouse gas emissions originate from the production and activation processes. In the case of wheat-based feedstock, emissions are primarily driven by fertilizer production for crop cultivation and energy consumption during straw processing. Substantial differences are also observed in water consumption, reaching 4.7 m^3 world-eq/kg for wheat, compared with 1.15 and 0.11 m^3 world-eq/kg for sawdust and coconut, respectively.

As indicated by a techno-economic analysis of different scenarios for activated carbon production based on biochar derived from waste biomass, annual OPEX costs are approximately 1.7–2.6 times lower than CAPEX, suggesting that the technology is moderately capital-intensive and may offer a favorable payback period.[123] The main CAPEX cost drivers include the activation unit, accounting for 39–49% of total capital costs, as well as the pyrolysis reactor and heat exchanger, each contributing up to approximately 20%. In terms of OPEX, despite the low cost and wide availability of waste biomass, high expenses associated with activating agents result in raw material-related costs exceeding 60% of total operating costs. Model calculations indicate that a 30% increase in feedstock cost leads to an increase in activated carbon production cost of nearly 17% points. Utility costs, including electricity and cooling water, also represent a significant component of OPEX; a 30% increase in these costs increases the activated carbon price by almost 9%. In contrast, fixed operating costs, including maintenance and labor, are relatively less high, accounting for approximately 12–17% of total OPEX.

Currently, the scientific literature has not thoroughly investigated the potential for repurposing spent or enriched adsorbents used to remove sulfur compounds from boiler flue gases, automotive exhausts, or biogas. However, as indicated by the techno-economic analysis presented in,[123] the use of waste biomass for the production of activated carbon can reduce the production cost of this material from the current €0.42/kg to approximately €0.13–0.24/kg. This cost is comparable to that of commonly used calcium-based sorbents (€0.20/kg[124]) and lower than that of ammonia (approximately €0.45/kg[125]), magnesium-based sorbents (€0.50/kg[126]), sodium-based sorbents (approximately €0.70/kg[127]), and amine solutions (€2.0/kg-[128]). The potential use of these as soil improvers/organic fertilizers remains unclear, despite the possibility that they could play a significant role in promoting sustainable resource management and minimizing waste. However, there is evidence that adding biochar to the soil can reduce the amount of fertilizer used, guaranteeing increased yields and lower production costs. Zhang et al. [129] conducted a three-year field study (2019–2021) in maize using biochar as a soil amendment at rates of 0, 8, 16, and 24 t/ha. Simultaneous nitrogen fertilizer application was carried out at rates of conventional N application (200 kg N/ha), a 20% reduction in N application (160 kg N/ha), and a 40% reduction in N application (120 kg N/ha). Biochar addition with 20% and 40% reduction in N fertilizer application was shown to improve maize growth, nitrogen uptake, and grain yield. Between 2019 and 2021, the addition of biochar increased maize grain yield by an average of 8.5%–18.4%, while economic benefits increased by 15.1%–18.4% between 2020 and 2021.

Research on activated carbons derived from bio-waste has yielded promising results in solving environmental challenges. In the context of diesel desulfurization, aimed at reducing SO_2 emissions from diesel engine combustion, the sugarcane bagasse bioadsorbent demonstrated high efficiency, achieving an adsorption capacity of 1.7 g/g of total sulfur. In comparison, the activated carbon and bentonite composite achieved a much lower adsorption value for dibenzothiophene – a key organo-sulfur compound present in diesel – of only 29 mg/g.[26] In the case of H_2S, rice straw biochar demonstrated an impressive adsorption level of 1.1 g/g from the gas stream,[28] confirming its potential in advanced gas purification technologies, similar to that of sugarcane bagasse bioadsorbent. Given the challenges of the high cost of activated carbon in the commercial industry the current market restrictions on the use of fossil fuels, advances in the development of cost-effective adsorbents whose production is compatible with the principles of a circular economy represent a promising and sustainable way forward. However, the biggest challenge remains the efficient conversion of waste into activated carbon, particularly when utilizing sulfur-rich biochar as a fertilizer. Guidelines detailing the manufacturing process and the feasibility of using biochar in precision agriculture are included in documents produced by the European Biochar Foundation (Switzerland), the British Biochar Foundation (UK) and the International Biochar Initiative (USA). These include the European Biochar Certificate (EBC) and the Biochar Quality Mandate (BQM). A project under the European Commission's 7th Framework Program, REFERTIL (Reducing the use of mineral fertilizers and chemicals in agriculture by recycling treated organic waste as compost and biochar products), led to the development of quality requirements for biochar. This document provides guidelines and recommendations to the European Commission intended for use in preparing fertilizer regulations.[130]

According to the EBC guidelines, biochar must fulfill certain conditions, such as a carbon content above 50% of the dry mass and a molar ratio of H/C_{org} less than 0.7. Additionally, depending on the application (e.g., agro, urban, consumer materials), biochar must meet different criteria, but it should be characterized in terms of elemental analysis (declaration of C_{tot}, C_{org}, H, N, O, S, ash), physical parameters (water content, dry matter (as received and <3 mm particle size), bulk density (d.m.), water holding capacity, pH, salt content, electrical conductivity of the solid biochar), thermogravimetric analysis, nutrients (declaration of N, P, K, Mg, Ca, Fe), heavy metals (Pb, Cd, Cu, Ni, Hg, Zn, Cr, As), organic contaminants (PAH, PCB, PCDD/F).[131] The IBI (International Biochar Initiative) guidelines, on the other hand, indicate that the heavy metal content of biochar should be within certain limits: mercury 1–17 mg/kg dry matter (d.m.), lead 121–300 mg/kg d.m., cadmium 1.4–39 mg/kg d.m., nickel 7–420 mg/kg d.m. and arsenic 13–100 mg/kg d.m. It should be noted that flue gas desulfurization processes using activated carbon, in addition to effectively removing SO_2, also adsorb some of the heavy metals. One of the most toxic heavy metals that can be adsorbed on activated carbon is mercury. Activated carbon shows the ability to adsorb both Hg^0 and its oxidized form Hg^{2+}. The flue gas desulfurization process also promotes the adsorption of other heavy metals such as Cd, Ni or Pb. According to Wang et al.[92] the maximum adsorption capacities of activated carbon for Hg^{2+}, Cd^{2+} and Ni^{2+} are 333 mg/g, 500 mg/g and 52.6 mg/g, respectively.

Activated carbon after sorption containing heavy metals can be toxic to soil and plants. Exceeding permissible standards for these elements may prevent their reuse or require stabilization methods. Although HgS is persistent under neutral and alkaline conditions, it can readily decompose in acidic or anaerobic environments, releasing toxic forms of mercury that migrate to groundwater and plants. To minimize the accumulation of mercury in activated carbon, consideration of its reuse, for example, as a fertilizer, should perhaps only apply to adsorbents from flue gas desulfurization plants where mercury removal has taken place at earlier stages. Such an approach would increase the recyclability of such activated carbon and minimize the environmental risks associated with its use. In particular, the key factor determining the safe use of biochar as a soil material is primarily the level of its physicochemical contaminants. The requirements and definitions established by biochar quality control bodies (voluntarily) are inconsistent and vary from standard to standard and from country to country.[130] Not all forms of sulfur are accessible to plants. Plants take up sulfur mainly in the form of SO_4^{2-} from the soil solution. In contrast, other forms of sulfur, such as elemental S^0 or S^{2-}, require microbial or chemical transformations, which, depending on soil conditions, can take up to several months.[132]

Importantly, according to the ECB guidelines, biochar is the material resulting from the pyrolysis of biomass, while it is not the material obtained from torrefaction or hydrothermal carbonization. The pyrolysis of bio-waste, carried out under anaerobic conditions, although an environmentally friendly alternative to traditional incineration, presents significant technological challenges. These include the control of CO_2, NO_x, and SO_x emissions resulting from the transformation of nitrogen and sulfur compounds present in the bio-waste,[133] as well as the formation of pyrolysis tar, which can deposit on reactor internals, reducing process efficiency and requiring additional cleaning procedures. The pyrolysis process is energy-intensive, necessitating the optimization of operational parameters. One solution is to recirculate the pyrolysis gases, allowing the heat generated to be reused for further waste decomposition. Combining this approach with pressure pyrolysis, although further optimization studies are needed, shows potential in reducing unwanted by-products and could further enhance the process.[134] Vacuum pyrolysis reduces the decomposition of biomass into greenhouse gases by providing better control over thermal processes. Additionally, reduced pressure can enhance the properties of biochar by increasing its porosity and sorption capacity, thereby making it more effective for environmental applications.[135,136] Integrating biomass pyrolysis with syngas production offers the possibility of obtaining hydrogen for industrial and energy applications, thereby supporting the concept of sustainability.[137,138]

The diversity of bio-waste is one of the challenges in the carbonization process, as it leads to variability in the properties of the resulting biochar. As shown in Table 1, different sources of biomass result in materials with varying sorption capacities, posing a challenge in standardizing their properties. This inconsistency not only makes it difficult to evaluate their effectiveness in industrial settings but also creates challenges in determining standardized pyrolysis conditions, which restricts the ability to produce results with reliable and uniform characteristics.

The biochars produced from the pyrolysis of biomass tend to have lower natural sorption activity, primarily due to their reduced porosity and the limited number of active sites available on their surface for interaction with gas molecules. Consequently, their capability for adsorbing gases like hydrogen sulfide or sulfur dioxide is inferior to that of commercially available activated carbons. The sorption properties of biochar can be enhanced by functionalizing its surface, either through physical activation with CO_2, chemical activation with KOH, or impregnation with metals (Cu, Fe, Zn). However, ensuring homogeneous quality of biochar on a large scale by pyrolysis of bio-waste involves high costs, which may make biochar production less cost-effective compared to fossil fuel-derived activated carbons already available on the market. Catalytic pyrolysis may offer a promising solution to the problems

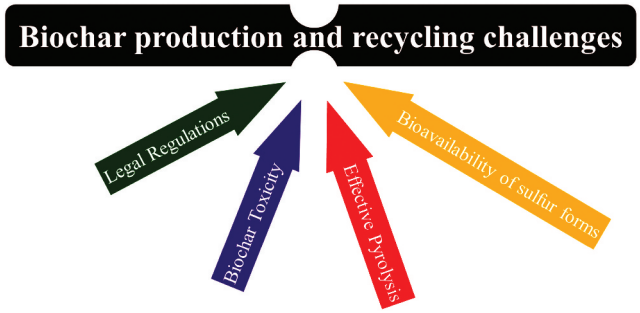

Figure 9. Challenges in the production of biochar and recycling of biochar after sulfur adsorption.

associated with traditional pyrolysis.[139] Catalysts can enhance the efficiency of biomass breakdown and regulate the reactions that produce coals with a more uniform chemical structure. Catalytic pyrolysis can facilitate more precise and controlled processes, minimizing undesirable by-products and boosting overall process efficiency.[140] Despite the promising benefits, the application of catalytic pyrolysis in biochar production requires further research, particularly in optimizing catalysts, catalyst regenerability and the cost of industrial-scale implementation. These catalysts must contribute to increased biochar production yields and improved pore decomposition. Mishra and Mohanty [141] showed that although the biochar obtained from neem seeds had a 63% concentration of elemental carbon, it had a low 4.6 m^2/g specific surface area.

In conclusion, before implementing the described technology in agricultural practice, further analyses are necessary to assess its safety and environmental impact. Biochars, which become a sulfur carrier after gas desulfurization, can increase sulfur availability to plants, supporting their growth and development. However, their potential use in precision agriculture presents some challenges (Figure 9). Regulations clarify which materials can be considered biochar and impose requirements for the biomass pyrolysis process. The fact that biochars may contain heavy metals is also a significant concern, necessitating thorough safety assessments before reuse. Ultimately, the form of sulfur in the biochar, its bioavailability and the way it is released into the soil are crucial to the effectiveness of this material as a fertilizer.

CONCLUSIONS

A model for a circular economy is proposed examining the dual use of bio-waste: first as a raw material for activated carbon and then as a soil fertilizer. It evaluates a concept in which biochars are returned to the soil as fertilizer and plants take up sulfur from the soil, closing the elemental cycle. The literature review has shown that biochars can be effective adsorbents for gases such as SO_2 and H_2S. The properties of the feedstock largely determine biochar efficiency – lignocellulosic materials produced at higher pyrolysis temperatures (≥500°C) exhibit a linearly increasing maximum sulfur adsorption with increasing pyrolysis temperature. In contrast, biochars derived from organo-mineral feedstocks show significantly lower efficiency regardless of the pyrolysis temperature.

The moisture content and particle size of raw materials have a significant impact on pyrolysis efficiency and the properties of the resulting biochar. Raw materials are typically dried in the 45–110°C range, often for ~24 h, with no optimal standards. Grinding reduces pyrolysis time, but increases energy consumption; particles used include both fine (<0.2 mm) and coarser (>30 mm) fractions. Biochars can be activated chemically with KOH or $ZnCl_2$ or physically with CO_2, steam, or O_2/N_2, to increase the surface area and sorption capacity. Pyrolysis is primarily carried out through slow pyrolysis at temperatures ranging from 400 to 600°C and times varying from a few minutes to a few hours, in an inert or oxygen-limited atmosphere. The effect of pyrolysis pressure and the use of slow pyrolysis remain insufficiently studied, representing significant gaps in practical knowledge.

Sulfur-enriched biochar shows significant potential as a soil amendment, serving both as an adsorbent and a fertilizer. The sulfur content and speciation in biochar depend primarily on the type of feedstock and the pyrolysis conditions, while additional sulfur enrichment can increase the number of active functional groups responsible for the sorption properties and reactivity of the material. Although the mechanism of sulfur release from biochar into soil is not yet fully understood, available studies indicate that sulfur is gradually converted into sulfate forms, which are readily available for plant uptake. Studies confirm its positive effects on crop yield, the availability of macro- and microelements, soil structure, water retention, and microbial activity. It may also enhance plant resistance to abiotic stresses and limit the development of pathogens through the activity of reactive oxygen and sulfur species. The use of biochar as fertilizer aligns with the concept of a circular economy; however, implementing this approach requires further field studies, evaluation of safety and economic feasibility, as well as the development of appropriate regulatory frameworks and market acceptance.

AUTHOR CONTRIBUTIONS

CRediT: **Anna M. Kisiela-Czajka:** Conceptualization, Formal analysis, Investigation, Supervision, Visualization, Writing – original draft, Writing – review & editing; **Temifemi Agbebunmi:** Conceptualization, Funding acquisition, Investigation, Visualization, Writing – original draft; **Krzysztof M. Czajka:** Conceptualization, Formal analysis, Investigation, Supervision, Visualization, Writing – original draft, Writing – review & editing; **Izabela Michalak:** Conceptualization, Formal analysis, Investigation, Supervision, Visualization, Writing – original draft, Writing – review & editing.

ACKNOWLEDGMENTS

Gratitude is extended to Freepik for providing access to free graphics. TA is grateful to the Erasmus Mundus Joint Master's Program, Sustainable Biomass and Bioproducts Engineering, Project 101050789 Sus2BioEng, for the financial support of her studies and research.

DISCLOSURE STATEMENT

All authors collaborated on and contributed to the entire manuscript and have given their consent to its publication.

FUNDNIG

The work was supported by the Erasmus Mundus Joint Master's Program, Sustainable Biomass and Bioproducts Engineering, [101050789] Sus2BioEng.

REFERENCES

[1] Hoesly, R. M.; Smith, S.; Prime, N.; Ahsan, H. A Global Anthropogenic Emissions Inventory of Reactive Gases and Aerosols (1750–2023): An Update to the Community Emissions Data System (CEDS) [Poster presentation]. AGU Fall Meeting 2024, Washington, D.C. United States, Dec 9–13, 2024.

[2] European Environment Agency. European Union Emission Inventory Report 1990-2021 – Under the UNECE Convention on Long-Range Transboundary Air Pollution (Air Convention). 2023. https://horizoneuropencpportal.eu/sites/default/files/2024-

05/eea-european-union-emission-inventory-report-1990-2021-2023_0.pdf.
[3] Li, C.; McLinden, C.; Fioletov, V.; Krotkov, N.; Carn, S.; Joiner, J.; Streets, D.; He, H.; Ren, X.; Li; Z., et al. India Is Overtaking China as the World's Largest Emitter of Anthropogenic Sulfur Dioxide. *Sci. Rep.* 2017, *7*(1), 14306. DOI: 10.1038/s41598-017-14639-8.
[4] Townsend-Small, A.; Edgar, A.; Fernandez, J. M.; Jackson, A.; Currit, N. High Rates of Hydrogen Sulfide Emissions Measured from Marginal Oil Wells Near Austin and San Antonio, Texas. *Environ. Res. Commun.* 2024, *6*(9), 091007. DOI: 10.1088/2515-7620/ad75f0.
[5] Zheng, B.; Tong, D.; Li, M.; Liu, F.; Hong, C.; Geng, G.; Li, H.; Li, X.; Peng, L.; Qi, J.; et al. Trends in China's Anthropogenic Emissions Since 2010 as the Consequence of Clean Air Actions. *Atmos. Chem. Phys.* 2018, *18*(19), 14095–14111. DOI: 10.5194/acp-18-14095-2018.
[6] Ni, T.; Wang, Y.; Huang, C.; Jiang, D.; Liu, Q. Limestone–Gypsum Wet Flue Gas Desulfurization Wastewater Treatment. *IOP Conf. Ser. Earth Environ. Sci.* 2021, *651*(4), 042034. DOI: 10.1088/1755-1315/651/4/042034.
[7] Milak, P.; Simao, L.; Daleffe, A.; Bergmann, C. P. Evaluation of Flue Gas Desulfurization (FGD) Waste Potentiality from Coal-Fired Power Plants to Obtain Alkali-Activated Materials. *Minerals* 2025, *15*(9), 930. DOI: 10.3390/min15090930.
[8] Czajka, K. M.; Kawalec, W.; Król, R.; Sówka, I. Modelling and Calculation of Raw Material Industry. *Energies* 2022, *15*(14), 5035. DOI: 10.3390/en15145035.
[9] Yaashikaa, P. R.; Kumar, P. S.; Varjani, S.; Saravanan, A. A Critical Review on the Biochar Production Techniques, Characterization, Stability and Applications for Circular Bioeconomy. *Biotechnol. Rep.* 2020, *28*, e00570. DOI: 10.1016/j.btre.2020.e00570.
[10] Xiao, Z.; Liu, Y.; Pan, J.; Wang, Y. Review of the Adsorption of Sulfur-Containing Gaseous Pollutants by Biochar: Progress, Challenges, and Perspectives. *Energy Fuels* 2025, *39*(9), 4151–4166. DOI: 10.1021/acs.energyfuels.4c06274.
[11] Choudhury, A.; Lansing, S. Adsorption of Hydrogen Sulfide in Biogas Using a Novel Iron-Impregnated Biochar Scrubbing System. *J. Environ. Chem. Eng.* 2021, *9*(1), 104837. DOI: 10.1016/j.jece.2020.104837.
[12] Chen, S.; Guo, Y.; Zhang, J.; Guo, Y.; Liang, X. CuFe2O4/Activated Carbon Adsorbents Enhance H_2S Adsorption and Catalytic Oxidation from Humidified Air at Room Temperature. *Chem. Eng. J.* 2022, *431*(Part 2), 134097. DOI: 10.1016/j.cej.2021.134097.
[13] Zhang, H.; Voroney, R. P.; Price, G. W.; White, A. J. Sulfur Enriched Biochar as a Potential Soil Amendment and Fertilizer. *Soil Res.* 2017, *55*(1), 93–99. DOI: 10.1071/SR15256.
[14] El-Sharkawy, M.; El-Naggar, A. H.; Al-Huqail, A. A.; Ghoneim, A. M. Acid-Modified Biochar Impacts on Soil Properties and Biochemical Characteristics of Crops Grown in Saline-Sodic Soils. *Sustainability* 2022, *14*(13), 8190. DOI: 10.3390/su14138190.
[15] Taheri, M. A. R.; Astaraei, A. R.; Lakzian, A.; Emami, H. The Role of Biochar and Ertili-Modified Biochar on Soil Water Content, Biochemical Properties and Millet Crop Under Saline-Sodic and Calcareous Soil. *Plant. Soil* 2023, *499*(1–2), 221–236. DOI: 10.1007/s11104-023-05912-z.
[16] Gholizadeh, M.; Meca, S.; Zhang, S.; Clarens, F.; Hu, X. Understanding the Dependence of Biochar Properties on Different Types of Biomass. *Waste Manage.* 2024, *182*, 142–163. DOI: 10.1016/j.wasman.2024.04.011.
[17] Hu, J.; Shang, R.; Heijman, B.; Rietveld, L. Reuse of Spent Granular Activated Carbon for Organic Micropollutant Removal from Treated Wastewater. *J. Environ. Manage.* 2015, *160*, 98–104. DOI: 10.1016/j.jenvman.2015.06.011.
[18] Fouda-Mbanga, B. G.; Onotu, O.; Tywabi-Ngeva, Z. Advantages of the Reuse of Spent Adsorbents and Potential Applications in Environmental Remediation: A Review. *Green Anal. Chem.* 2024, *11*, 100156. DOI: 10.1016/j.greeac.2024.100156.
[19] Nthwane, Y. B.; Fouda-Mbanga, B. G.; Thwala, M.; Pillay, K. A Comprehensive Review of Heavy Metals (Pb^{2+}, Cd^{2+}, Ni^{2+}) Removal from Wastewater Using Low-Cost Adsorbents and Possible Fertilizer Ion of Spent Adsorbents in Blood Fingerprint Application. *Environ. Technol.* 2023, *46*(3), 414–430. DOI: 10.1080/09593330.2024.2358450.
[20] Fouda-Mbanga, B. G.; Velempini, T.; Pillay, K.; Tywabi-Ngeva, Z. Heavy Metals Removals from Wastewater and Reuse of the Metal Loaded Adsorbents in Various Applications: A Review. *Hybrid Adv.* 2024, *6*, 100193. DOI: 10.1016/j.hybadv.2024.100193.
[21] Yang, W.; Zheng, X.; Cao, M. The Reuse Potential of Spent ZIF-8@GO-COOH Nano Adsorption Materials: Study on Their Impact on the Hydration Mechanism and Mechanical Properties of Cement-Based Composites. *Constr. Build Mater.* 2023, *387*, 131667. DOI: 10.1016/j.conbuildmat.2023.131667.
[22] Simon, D.; Gass, S.; Quaranta, N.; Cristobal, A. Production of Fired Clay Bricks as a Safe Removal Method for Spent Adsorbents from Sunflower and Corn Residues. *J Clean Prod.* 2023, *426*, 139138. DOI: 10.1016/j.jclepro.2023.139138.
[23] Arunachellan, I. C.; Bhaumik, M.; Brink, H. G.; Pillay, K.; Maity, A. Efficient Aqueous Copper Removal by Burnt Tire-Derived Carbon-Based Nanostructures and Their Utilization as Catalysts. *Minerals* 2024, *14*(3), 302. DOI: 10.3390/min14030302.
[24] Izhar, T. N. T.; Kee, G. Z.; Saad, F. N. M.; Rahim, S. Z. A.; Zakarya, I. A.; Besom, M. R. C.; Ibad, M.; Syafiuddin, A. Adsorption of Hydrogen Sulfide (H_2S) from Municipal Solid Waste by Using Biochars. *Biointerface Res. Appl. Chem.* 2022, *12*, 8057–8069. DOI: 10.33263/BRIAC126.80578069.
[25] Zhao, B.; Xu, H.; Ma, F.; Zhang, T.; Nan, X. Effects of Dairy Manure Biochar on Adsorption of Sulfate onto Light Sierozem and Its Mechanisms. *RSC Adv.* 2019, *9*, 5218–5223. DOI: 10.1039/c8ra08916g.
[26] Golnari, K.; Alijani, H.; Nobakht, V.; Mokhtari, B. High-Performance Total Sulfur Removal from Diesel Fuel Using Amine Functionalized Biochar: Equilibrium, Kinetic Study and Experimental Design. *Chem. Eng. Res. Des.* 2022, *185*, 253–266. DOI: 10.1016/j.cherd.2022.07.006.
[27] Su, L.; Chen, M.; Zhuo, G.; Ji, R.; Wang, S.; Zhang, L.; Zhang, M.; Li, H. Comparison of Biochar Materials Derived from Coconut Husks and Various Types of Livestock Manure, and Their Potential for Use in Removal of H_2S from Biogas. *Sustainability* 2021, *13*(11), 6262. DOI: 10.3390/su13116262.
[28] Zhao, Y.; Liu, Y. Preparation of Hydrogen Sulfide Adsorbent Derived from Spent Fenton-Like Reagent Modified Biochar and Its Removal Characteristics for Hydrogen Sulfide. *Fuel Process. Technol.* 2022, *238*, 107495. DOI: 10.1016/j.fuproc.2022.107495.
[29] Juntarachat, N.; Onthong, U. Removal of Hydrogen Sulfide from Biogas Using Banana Peel and Banana Empty Fruit Bunch Biochars as Alternative Adsorbents. *Biomass Convers Biorefin.* 2024, *14*(21), 27077–27088. DOI: 10.1007/s13399-022-03430-z.
[30] Baikousi, M.; Gantzoudi, A.; Gioti, C.; Moschovas, D.; Giannakas, A.; Avgeropoulos, A.; Salmas, C. E.; Karakassides, M. H_2S Removal via Sorption Process on Activated Carbon-Metal Oxide Composites Derived from Different Biomass Sources. *Molecules* 2023, *28*(21), 7418. DOI: 10.20944/preprints202310.0308.v1.
[31] Shang, G.; Shen, G.; Wang, T.; Chen, Q. Effectiveness and Mechanisms of Hydrogen Sulfide Adsorption by Camphor-Derived Biochar. *J. Air Waste Manage. Assoc.* 2012, *62*(8), 873–879. DOI: 10.1080/10962247.2012.686441.
[32] Hervy, M.; Pham Minh, D.; Gerente, C.; Weiss-Hortala, E.; Nzihou, A.; Villot, A.; Le Coq, L.; Gérente, C. Removal from Syngas Using Wastes Pyrolysis Chars. *Chem. Eng. J.* 2018, *334*, 2179–2189. DOI: 10.1016/j.cej.2017.11.162.
[33] Sawalha, H.; Maghalseh, M.; Qutaina, J.; Junaidi, K.; Rene, E. R. Removal of Hydrogen Sulfide from Biogas Using Activated Carbon Synthesized from Different Locally Available Biomass Wastes - A Case Study from Palestine. *J. Environ. Sci. Health* 2020, *11*(1), 607–618. DOI: 10.1080/21655979.2020.1768736.
[34] Ro, K. S.; Woodbury, B.; Spiehs, M.; Szogi, A. A.; Silva, P. J.; Hwang, O.; Cho, S. Pilot-Scale H_2S and Swine Odor Removal System Using Commercially Available Biochar. *Agronomy* 2021, *11*(8), 1611. DOI: 10.3390/agronomy11081611.

[35] Braghiroli, F. L.; Bouafif, H.; Koubaa, A. Enhanced SO_2 Adsorption and Desorption on Chemically and Physically Activated Biochar Made from Wood Residues. *Ind. Crops Prod.* 2019, *138*, 111500. DOI: 10.1016/j.indcrop.2019.06.019.
[36] Sanchez-Borrego, F. J.; García-Criado, N.; García-Martín, J. F.; Álvarez-Mateos, P. Determination of the Composition of Bio-Oils from the Pyrolysis of Orange Waste and Orange Pruning and Use of Biochars for the Removal of Fertilizer from Waste Cooking Oils. *Agronomy* 2022, *12*(2), 309. DOI: 10.3390/agronomy12020309.
[37] Sun, Y.; Yang, G.; Zhang, L.; Sun, Z. Preparation of High Performance H2S Removal Biochar by Direct Fluidized Bed Carbonization Using Potato Peel Waste. *Process Saf. Environ. Prot.* 2017, *107*, 281–288. DOI: 10.1016/j.psep.2017.02.018.
[38] Iberahim, N.; Sethupathi, S.; Bashir, M. J. K.; Kanthasamy, R.; Ahmad, T. Evaluation of Oil Palm Fiber Biochar and Activated Biochar for Fertilizer Dioxide Adsorption. *Sci. Total Environ.* 2022, *805*, 150421. DOI: 10.1016/j.scitotenv.2021.150421.
[39] Nowicki, P.; Skibiszewska, P.; Pietrzak, R. Hydrogen Sulphide Removal on Carbonaceous Adsorbents Prepared from Coffee Industry Waste Materials. *Chem. Eng. J.* 2014, *248*, 208–215. DOI: 10.1016/j.cej.2014.03.052.
[40] Junior, A.; Guo, M. Efficacy of Sewage Sludge Derived Biochar on Enhancing Soil Health and Crop Productivity in Strongly Acidic Soil. *Front. Soil Sci.* 2023, *3*, 1066547. DOI: 10.3389/fsoil.2023.1066547.
[41] Iberahim, N.; Sethupathi, S.; Bashir, M. J. K.; Kanthasamy, R.; Ahmad, T. Optimization of Activated Palm Oil Sludge Biochar Preparation for Fertilizer Dioxide Adsorption. *J. Environ. Manag.* 2019, *248*, 109302. DOI: 10.1016/j.jenvman.2019.109302.
[42] Xu, S.; Deng, W.; Hu, M.; Chen, G.; Zhou, P.; Li, F.; Su, Y. Preparation of Activated Sludge Char Through Microwave-Assisted One-Step Pyrolysis and Activation for Gaseous H_2S Removal. *Chem. Eng. Process. Process Intensif.* 2022, *181*, 109175. DOI: 10.1016/j.cep.2022.109175.
[43] Gaga, Y.; Benmessaoud, S.; Kara, M.; Assouguem, A.; Al-Ghamdi, A. A.; Al-Hemaid, F. M.; Elshikh, M. S.; Ullah, R.; Banach, A.; Bahhou, J. New Margin-Based Biochar for Removing Hydrogen Sulfide Generated During the Anaerobic Wastewater Treatment. *Water* 2022, *14*(20), 3319. DOI: 10.3390/w14203319.
[44] Iberahim, N.; Sethupathi, S.; Bashir, M. J. K. Optimization of Palm Oil Mill Sludge Biochar Preparation for Sulfur Dioxide Removal. *Environ. Sci. Pollut. Res.* 2018, *25*(26), 25702–25714. DOI: 10.1007/s11356-017-9180-5.
[45] Sahota, S.; Vijay, V. K.; Subbarao, P. M. V.; Chandra, R.; Ghosh, P.; Shah, G.; Kapoor, R.; Vijay, V.; Koutu, V.; Thakur, I. S. Characterization of Leaf Waste Based Biochar for Cost Effective Hydrogen Sulphide Removal from Biogas. *Bioresour. Technol.* 2018, *250*, 635–641. DOI: 10.1016/j.biortech.2017.11.093.
[46] Han, X.; Chen, H.; Liu, Y.; Pan, J. Study on Removal of Gaseous Hydrogen Sulfide Based on Macroalgae Biochars. *J. Nat. Gas Sci. Eng.* 2020, *73*, 103068. DOI: 10.1016/j.jngse.2019.103068.
[47] Dou, Z.; Chen, H.; Liu, Y.; Huang, R.; Pan, J. Removal of Gaseous H_2S Using Microalgae Porous Carbons Synthesized by Thermal/Microwave KOH Activation. *J. Energy. Inst.* 2022, *101*, 45–55. DOI: 10.1016/j.joei.2021.12.007.
[48] Chun, Y.; Lee, S. K.; Yoo, H. Y.; Kim, S. W. Recent Advancements in Biochar Production According to Feedstock Classification, Pyrolysis Conditions, and Applications: A Review. *BioResources* 2021, *16*(3), 6512–6547. DOI: 10.15376/biores.16.3.Chun.
[49] Qin, L.; Wu, Y.; Hou, Z.; Jiang, E. Influence of Biomass Components, Temperature and Pressure on the Pyrolysis Behavior and Biochar Properties of Pine Nut Shells. *Bioresour. Technol.* 2020, *323*, 123682. DOI: 10.1016/j.biortech.2020.123682.
[50] Xiong, S.; Zhuo, J.; Zhang, B.; Yao, Q. Effect of Moisture Content on the Characterization of Products from the Pyrolysis of Sewage Sludge. *J. Anal. Appl. Pyrolysis* 2013, *104*, 632–639. DOI: 10.1016/j.jaap.2013.05.003.
[51] Domínguez, A.; Menéndez, J. A.; Pis, J. J. Hydrogen Rich Fuel Gas Production from the Pyrolysis of Wet Sewage Sludge at High Temperature. *J. Anal. Appl. Pyrolysis* 2006, *77*(2), 127–132. DOI: 10.1016/j.jaap.2006.02.003.
[52] Domínguez, A.; Fernández, Y.; Fidalgo, B.; Pis, J. J.; Menéndez, J. A. Bio-Syngas Production With Low Concentrations of CO_2 and CH_4 From Microwave-Induced Pyrolysis of Wet and Dried Sewage Sludge. *Chemosphere* 2008, *70*(3), 397–403. DOI: 10.1016/j.chemosphere.2007.06.075.
[53] Zhang, B.; Xiong, S.; Xiao, B.; Yu, D.; Jia, X. Mechanism of Wet Sewage Sludge Pyrolysis in a Tubular Furnace. *Int. J. Hydrogen Energy* 2011, *36*(1), 355–363. DOI: 10.1016/j.ijhydene.2010.05.100.
[54] Liu, S.; Zhang, G.; Bi, D.; Ni, Y.; Song, J.; Song, X.; Wang, H. Effect of Pyrolysis Conditions on the Preparation of Nitrogen-Containing Chemicals and Nitrogen-Doped Carbon from Cock Feathers: Nitrogen Migration and Transformation. *Energy* 2025, *315*, 134328. DOI: 10.1016/j.energy.2024.134328.
[55] Hossain, M. Z.; Bahar, M. M.; Sarkar, B.; Donne, S. W.; Ok, Y. S.; Palansooriya, K. N.; Kirkham, M. B.; Chowdhury, S.; Bolan, N. Biochar and Its Importance on Nutrient Dynamics in Soil and Plant. *Biochar* 2020, *2*(4), 379–420. DOI: 10.1007/s42773-020-00065-z.
[56] Xu, X.; Huang, D.; Zhao, L.; Kan, Y.; Cao, X. Role of Inherent Inorganic Constituents in SO_2 Sorption Ability of Biochars Derived from Three Biomass Wastes. *Environ. Sci. Technol.* 2016, *50*(23), 12957–12965. DOI: 10.1021/acs.est.6b03077.
[57] Al-Rabaiai, A.; Menezes-Blackburn, D.; Al-Ismaily, S.; Janke, R.; Al-Alawi, A.; Al-Kindi, M.; Bol, R. Biochar pH Reduction Using Elemental Sulfur and Biological Activation Using Compost or Vermicompost. *Bioresour. Technol.* 2024, *401*, 130707. DOI: 10.1016/j.biortech.2024.130707.
[58] Makowska, M.; Dziosa, K. Influence of Different Pyrolysis Temperatures on Chemical Composition and Graphite-Like Structure of Biochar Produced from Biomass of Green Microalgae *Chlorella* sp. *Environ. Technol. Innovations* 2024, *35*, 103667. DOI: 10.1016/j.eti.2024.103667.
[59] Cai, N.; Zhang, H.; Nie, J.; Deng, Y.; Baeyens, J. Biochar from Biomass Slow Pyrolysis. *IOP Conf. Ser. Earth Environ. Sci.* 2020, *586*(1), 012001. DOI: 10.1088/1755-1315/586/1/012001.
[60] Zhang, J.; Liu, J.; Liu, R. Effects of Pyrolysis Temperature and Heating Time on Biochar Obtained from the Pyrolysis of Straw and Lignosulfonate. *Bioresour. Technol.* 2015, *176*, 288–291. DOI: 10.1016/j.biortech.2014.11.011.
[61] Chandra, S.; Bhattacharya, J. Influence of Temperature and Duration of Pyrolysis on the Property Heterogeneity of Rice Straw Biochar and Optimization of Pyrolysis Conditions for Its Application in Soils. *J. Clean Prod.* 2019, *215*, 1123–1139. DOI: 10.1016/j.jclepro.2019.01.079.
[62] Zhao, B.; Xu, H.; Zhang, T.; Nan, X.; Ma, F. Effect of Pyrolysis Temperature on Sulfur Content, Extractable Fraction and Release of Sulfate in Corn Straw Biochar. *RSC Adv.* 2018, *8*(62), 35611. DOI: 10.1039/c8ra06382f.
[63] Czajczyńska, D.; Czajka, K. M.; Krzyżyńska, R.; Jouhara, H. Experimental Analysis of Waste Tyres as a Sustainable Source of Energy. *E3S Web. Conf.* 2019, *100*, 00012. DOI: 10.1051/e3sconf/201910000012.
[64] Phadtare, P.; Kalbande, S. Biochar Production Technologies from Agricultural Waste, Its Utilization in Agriculture and Current Global Biochar Market: A Comprehensive Review. *Int. J. Environ. Clim. Change* 2022, *12*, 1010–1031. DOI: 10.9734/ijecc/2022/v12i1131078.
[65] Ali, S. A.; Saeed, S. M. G.; Ejaz, U.; Baloch, M. N.; Sohail, M. A Novel Approach to Improve the Nutritional Value of Black Gram (*Vigna Mungo* L.) by the Combined Effect of Pre-Gelatinization and Fermentation by *Lactobacillus* sp. E14 and *Saccharomyces Cerevisiae* MK-157: Impact on Morphological, Thermal, and Chemical Structural Properties. *LWT* 2022, *172*, 114216. DOI: 10.1016/j.lwt.2022.114216.
[66] Amalina, F.; Razak, A. S. A.; Krishnan, S.; Sulaiman, H.; Zularisam, A. W.; Nasrullah, M. Biochar Production Techniques Utilizing Biomass Waste-Derived Materials and Environmental Applications – A Review. *J. Hazard. Mater. Adv.* 2022, *7*, 100134. DOI: 10.1016/j.hazadv.2022.100134.
[67] Jayaraman, K.; Gokalp, I.; Petrus, S.; Belandria, V.; Bostyn, S. Energy Recovery Analysis from Sugar Cane Bagasse Pyrolysis

and Gasification Using Thermogravimetry, Mass Spectrometry and Kinetic Models. *J. Anal. Appl. Pyrolysis* 2018, *132*, 225–236. DOI: 10.1016/j.jaap.2018.02.003 .

[68] Ahmed, M. M. M.; Liao, C. H.; Venkatesan, S.; Liu, Y. T.; Tzou, Y. M.; Jien, S. H.; Lin, M. C.; Hsieh, Y. C.; Osman, A. I. Sulfur-Functionalized Sawdust Biochar for Enhanced Cadmium Adsorption and Environmental Remediation: A Multidisciplinary Approach and Density Functional Theory Insights. *J. Environ. Manage.* 2025, *373*, 123586. DOI: 10.1016/j.jenvman.2024.123586 .

[69] Ding, S.; Li, Y.; Zhu, T.; Guo, Y. Regeneration Performance and Carbon Consumption of Semi-Coke and Activated Coke for SO_2 and NO Removal. *J. Environ. Sci.* 2015, *34*, 37–43. DOI: 10.1016/j.jes.2015.02.004.

[70] Peterson, S.; Jackson, M. Simplifying Pyrolysis: Using Gasification to Produce Corn Stover and Wheat Straw Biochar for Sorptive and Horticultural Media. *Ind. Crops Prod.* 2014, *53*, 228–235. DOI: 10.1016/j.indcrop.2013.12.028.

[71] Shoaib, M.; Al-Swadian, H. Optimization and Characterization of Sliced Activated Carbon Prepared from Date Palm Tree Fronds by Physical Activation. *Biomass Bioenergy* 2015, *73*, 124–134. DOI: 10.1016/j.biombioe.2014.12.016.

[72] Yuan, H.; Lu, T.; Wang, Y.; Huang, H.; Cheng, Y. Influence of Pyrolysis Temperature and Holding Time on Properties of Biochar Derived from Medicinal Herb (*Radix Isatidis*) Residue and Its Effect on Soil CO_2 Emission. *J. Anal. Appl. Pyrolysis* 2014, *110*, 277–284. DOI: 10.1016/j.jaap.2014.09.016.

[73] Wang, Y.; Fan, C.; Hu, H.; Li, Y.; Sun, D.; Wang, Y.; Peng, L. Genetic Modification of Plant Cell Walls to Enhance Biomass Yield and Biofuel Production in Bioenergy Crops. *Biotechnol. Adv.* 2016, *34* (5), 997–1017. DOI: 10.1016/j.biotechadv.2016.06.001.

[74] Cui, X.; Yi, H.; Tang, X.; Zhao, S.; Yang, K.; Yan, B.; Li, C.; Yang, X.; Feng, T.; Ma, Y. Study of the Properties of Adsorption of SO_2 – Thermal Regeneration Cycle of Activated Coke Modified by Oxidization. *J. Chem. Technol. Biotechnol.* 2018, *93*(3), 720–729. DOI: 10.1002/jctb.5421.

[75] Atanes, E.; Nieto-Márquez, A.; Cambra, A.; Ruiz-Pérez, M.; Fernández-Martínez, F. Adsorption of SO_2 onto Waste Cork Powder-Derived Activated Carbons. *Chem. Eng. J.* 2012, *211–212*, 60–67. DOI: 10.1016/j.cej.2012.09.043.

[76] Lee, Y.; Park, J.; Choung, J.; Choi, D. Adsorption Characteristics of SO_2 on Activated Carbon Prepared from Coconut Shell with Potassium Hydroxide Activation. *Environ. Sci. Technol.* 2002, *36*, 1086–1092. DOI: 10.1021/es010916l.

[77] Zhu, Y.; Gao, J.; Li, Y.; Sun, F.; Gao, J.; Wu, S.; Qin, Y. Preparation of Activated Carbons for SO_2 Adsorption by CO_2 and Steam Activation. *J. Taiwan Inst. Chem. Eng.* 2012, *43*, 112–119. DOI: 10.1016/j.jtice.2011.06.009.

[78] Bonelli, P. R.; Buonomo, E. L.; Cukierman, A. L. Pyrolysis of Sugarcane Bagasse and Co-Pyrolysis with an Argentinean Subbituminous Coal. *Energy Sources A* 2007, *29*(8), 731–740. DOI: 10.1080/00908310500281247.

[79] Katyal, S.; Thambimuthu, K.; Valix, M. Carbonisation of Bagasse in a Fixed Bed Reactor: Influence of Process Variables on Char Yield and Characteristics. *Renewable Energy.* 2003, *28*(5), 713–725. DOI: 10.1016/S0960-1481(02)00112-X.

[80] Liu, W.; Adanur, S. Desulfurization Properties of Modified Activated Carbon Fibers and Activated Carbon Fiber Paper. *J. Ind. Text.* 2015, *44*(4), 513–525. DOI: 10.1177/152808371350.

[81] Wijitkosum, S.; Jiwnok, P. Elemental Composition of Biochar Obtained from Agricultural Waste for Soil Amendment and Carbon Sequestration. *Appl. Sci.* 2019, *9*(19), 3980. DOI: 10.3390/app9193980.

[82] Brunauer, S.; Emmet, P. H. The Use of Low Temperature Van Der Waals Adsorption Isotherms in Determining the Surface Areas of Various Adsorbents. *J. Am. Chem. Soc.* 1937, *59*(12), 2682–2689. DOI: 10.1021/ja01291a060.

[83] Kisiela-Czajka, A. M. Adsorption Behavior of SO_2 Molecules on Unburned Carbon from Lignite Fly Ash in the Context of Developing Commercially Applicable Environmental Carbon Adsorbent. *Energy* 2022, *250*, 123741. DOI: 10.1016/j.energy.2022.123741.

[84] Qu, Z.; Sun, F.; Gao, J.; Pi, X.; Qie, Z.; Zhao, G. A New Insight Into SO_2 Low-Temperature Catalytic Oxidation in Porous Carbon Materials: Non-Dissociated O_2 Molecule as Oxidant. *Catal. Sci. Technol.* 2019, *9*, 4327–4338. DOI: 10.1039/C9CY00960D.

[85] Lizzio, A. A.; DeBarr, J. A. The Mechanism of SO_2 Removal by Carbon. *Energy Fuels* 1997, *11*, 284–291. DOI: 10.1021/ef960197+.

[86] Jing, W.; Guo, Q.; Hou, Y.; Han, X.; Huang, Z. Study of SO_2 Oxidation Over V_2O_5/Activated Carbon Catalyst Using in situ Diffuse Reflectance Infrared Fourier Transformation Spectroscopy. *Korean J. Chem. Eng.* 2014, *31*(5), 794–800. DOI: 10.1007/s11814-013-0270-x.

[87] Yamamoto, T.; Tayakout-Fayolle, M.; Geantet, C. Gas-Phase Removal of Hydrogen Sulfide Using Iron Oxyhydroxide at Low Temperature: Measurement of Breakthrough Curve and Modelling of Sulfidation Mechanism. *Chem. Eng. J.* 2015, *262*, 702–709. DOI: 10.1016/j.cej.2014.09.093.

[88] Bottani, E. J.; Tascón, J. M. D. *Adsorption by Carbons*; Elsevier Science: Amsterdam, 2008. DOI: 10.1016/B978-0-08-044464-2.X5001-9.

[89] Richter, E. Carbon Catalysts for Pollution Control. *Catal. Today* 1990, *7*(2), 93–112. DOI: 10.1016/0920-5861(90)85011-C.

[90] Izquierdo, M. T.; Rubio, B. Carbon-Enriched Coal Fly Ash as a Precursor of Activated Carbons for SO_2 Removal. *J. Hazard. Mater.* 2008, *155*(1–2), 199–205. DOI: 10.1016/j.jhazmat.2007.11.047.

[91] Jacobs, J. H.; Chou, N.; Lesage, K. L.; Xiao, Y.; Hill, J. M.; Marriott, R. A. Investigating Activated Carbons for SO_2 Adsorption in Wet Flue Gas. *Fuel* 2023, *353*, 129239. DOI: 10.1016/j.fuel.2023.129239.

[92] Wang, Y.; Qi, T.; Hu, M.; Yang, Y.; Xing, L.; Wang, L. Simultaneous Catalysis of Sulfite Oxidation and Uptake of Heavy Metals by Bifunctional Activated Carbon Fiber in Magnesia Desulfurization. *Catalysts* 2020, *10*(2), 244. DOI: 10.3390/catal10020244.

[93] Annurov, S. A. Physicochemical Aspects of the Adsorption of Sulfur Dioxide by Carbon Adsorbents. *Russ. Chem. Rev.* 1996, *65* (8), 663–676. DOI: 10.1070/RC1996v065n08ABEH000221.

[94] Lisovskii, A.; Semiat, R.; Aharoni, C. Adsorption of Sulfur Dioxide by Active Carbon Treated by Nitric Acid: I. Effect of the Treatment on Adsorption of SO_2 and Extrability of the Acid Formed. *Carbon* 1997, *35*(10–11), 1639–1643. DOI: 10.1016/S0008-6223(97)00129-2.

[95] Yang, J. H. Hydrogen Sulfide Removal Technology: A Focused Review on Adsorption and Catalytic Oxidation. *Korean J. Chem. Eng.* 2021, *38*(4), 674–691. DOI: 10.1007/s11814-021-0755-y.

[96] Raymundo-Pinero, E.; Cazorla-Amoros, D.; Linares-Solano, A. The Role of Different Nitrogen Functional Groups on the Removal of SO_2 from Flue Gases by N-Doped Activated Carbon Powders and Fibres. *Carbon* 2003, *41*(10), 1925–1932. DOI: 10.1016/S0008-6223(03)00180-5.

[97] Moreno-Castilla, C.; Carrasco-Martin, F.; Utrera-Hidalgo, E.; Rivera-Ultrilla, J. Activated Carbons as Adsorbents of SO_2 in Flowing Air. Effect of Their Pore Texture and Surface Basicity. *Langmuir* 1993, *9*(5), 1378–1383. DOI: 10.1021/la00029a035.

[98] Wang, Q.; Han, L.; Wang, Y.; He, Z.; Meng, Q.; Wang, S.; Xiao, P.; Jia, X. Conversion of Coal Into N-Doped Porous Carbon for High-Performance SO_2 Adsorption. *RSC Adv.* 2022, *12*(32), 20640–20648. DOI: 10.1039/D2RA03098E.

[99] Bansal, R. C.; Goyal, M. *Activated Carbon Adsorption*; CRC Press: Boca Raton, 2005. DOI: 10.1201/9781420028812.

[100] Davini, P. Adsorption and Desorption of SO_2 on Active Carbon: The Effect of Surface Oxygen Groups. *Carbon* 1990, *28*(4), 565–571. DOI: 10.1016/0008-6223(90)90054-3.

[101] Davini, P. Adsorption of SO_2 on Thermally Treated Active Carbon. *Fuel* 1989, *68*(2), 145–148. DOI: 10.1016/0016-2361(89)90314-1.

[102] Cen, W.; Hou, M.; Liu, J.; Yuan, S.; Liu, Y.; Chu, Y. Oxidation of SO_2 and NO by Epoxy Groups on Graphene Oxides: The Role of the Hydroxyl Group. *RSC Adv.* 2015, *5*(29), 22802–22810. DOI: 10.1039/C4RA15179H.

[103] El-Naggar, A.; El-Naggar, A. H.; Shaheen, S. M.; Sarkar, B.; Chang, S. X.; Tsang, D. C. W.; Rinklebe, J.; Ok, Y. S. Biochar Composition-Dependent Impacts on Soil Nutrient Release, Carbon Mineralization, and Potential Environmental Risk: A Review. *J. Environ. Manage.* 2019, *241*, 458–467. DOI: 10.1016/j.jenvman.2019.02.044.

[104] Kizito, S.; Luo, H. Z.; Lu, J. X.; Bah, H.; Dong, R. J.; Wu, S. B. Role of Nutrient-Enriched Biochar as a Soil Amendment During Maize Growth: Exploring Practical Alternatives to Recycle Agricultural Residuals and to Reduce Chemical Fertilizer Demand. *Sustainability* 2019, *11*(11), 3211. DOI: 10.3390/su11113211.

[105] Pathak, S. K.; Singh, S.; Rajput, V. D.; Shan, S. D.; Srivastava, S. Sulfur-Modified Tea-Waste Biochar Improves Rice Growth in Arsenic Contaminated Soil and Reduces Arsenic Accumulation. *IScience* 2024, *27*(12), 111445. DOI: 10.1016/j.isci.2024.111445.

[106] Peng, Y.; Su, L.; Liu, M.; Zeng, C.; Xiang, B.; Xie, Z.; Hu, Z.; Zhou, N. Biochar-Enhanced Sulfur: Mechanistic Insights into a Novel and Effective Bactericide. *Nanomaterials* 2025, *15*(9), 697. DOI: 10.3390/nano15090697.

[107] Wu, C.; Shi, L.; Xue, S.; Li, W.; Jiang, X.; Rajendran, M.; Qian, Z. Effect of Sulfur-Iron Modified Biochar on the Available Cadmium and Bacterial Community Structure in Contaminated Soils. *Sci. Total Environ.* 2019, *647*, 1158–1168. DOI: 10.1016/j.scitotenv.2018.08.087.

[108] Agbebunmi, T.; Kisiela-Czajka, A. M.; Czajka, K. M.; Michalak, I. Valorization of Food Waste Biomass into Sulfur-Enriched Biochar: A Promising Step Towards Environmental Protection and Sustainable Agriculture. *Biomass Bioenergy.* 2026, *213*, 109452. DOI: 10.1016/j.biombioe.2026.109452.

[109] Leng, L.; Liu, R.; Xu, S.; Mohamed, B. A.; Yang, Z.; Hu, Y.; Chen, J.; Zhao, S.; Wu, Z.; Peng, H.; et al. An Overview of Sulfur-Functional Groups in Biochar from Pyrolysis of Biomass. *J. Environ. Chem. Eng.* 2022, *10*(2), 107185. DOI: 10.1016/j.jece.2022.107185.

[110] Cheah, S.; Malone, S. C.; Feik, C. J. Speciation of Sulfur in Biochar Produced from Pyrolysis and Gasification of Oak and Corn Stover. *Environ. Sci. Technol.* 2014, *48*(15), 8474–8480. DOI: 10.1021/es500073r.

[111] Yin, M.; Bai, X.; Wu, D.; Li, F.; Jiang, K.; Ma, N.; Chen, Z.; Zhang, X.; Fang, L. Sulfur-Functional Group Tuning on Biochar Through Sodium Thiosulfate Modified Molten Salt Process for Efficient Heavy Metal Adsorption. *Chem. Eng. J.* 2022, *433*(1), 134441. DOI: 10.1016/j.cej.2021.134441.

[112] Ahmed, M. M. M.; Liao, C.-H.; Liu, Y.-T.; Venkatesan, S.; Hsieh, Y.-C.; Nail, H. M.; Wang, H.-M. D.; Lin, M.-C.; Jien, S.-H.; Tzou, Y.-M. Sulfur-Functionalized Rice Straw Biochar for Enhanced Cadmium Sorption: Spectroscopic, Kinetic and Computational Insights. *J. Cleaner Prod.* 2024, *484*, 144267. DOI: 10.1016/j.jclepro.2024.144267.

[113] Churka Blum, S.; Lehmann, J.; Solomon, D.; Caires, E. F.; Alleoni, L. R. F. Sulfur Forms in Organic Substrates Affecting S Mineralization in Soil. *Geoderma* 2013, *200–201*, 156–164. DOI: 10.1016/j.geoderma.2013.02.003.

[114] Zimmer, D.; Panten, K.; Frank, M.; Springer, A.; Leinweber, P. Sulfur-Enriched Bone Char as Alternative P Fertilizer: Spectroscopic, Wet Chemical, and Yield Response Evaluation. *Agriculture* 2019, *9*(1), 21. DOI: 10.3390/agriculture9010021.

[115] Domingues, R. R.; Trugilho, P. F.; Silva, C. A.; Melo, I. C. N. A. D.; Melo, L. C. A.; Magriotis, Z. M.; Sánchez-Monedero, M. A. Properties of Biochar Derived from Wood and High-Nutrient Biomasses with the Aim of Agronomic and Environmental Benefits. *PLOS ONE* 2017, *12*(5), e0176884. DOI: 10.1371/journal.pone.0176884.

[116] Oyebamiji, Y. O.; Adigun, B. A.; Shamsudin, N. A. A.; Ikmal, A. M.; Salisu, M. A.; Malike, F. A.; Lateef, A. A. Recent Advancements in Mitigating Abiotic Stresses in Crops. *Horticulturae* 2024, *10*(2), 156. DOI: 10.3390/horticulturae10020156.

[117] Michalak, I.; Warchoł, J. Remediation of Soil Contaminated with Heavy Metals by Immobilization with Organic and Inorganic Amendments. In *Modern Approaches in Waste Bioremediation - Environmental Microbiology*, Shah, M. P., Ed.; Cham: Springer, 2023; pp. 181–210. DOI: 10.1007/978-3-031-24086-7_10.

[118] Zhao, B.; O'Connor, D.; Shen, Z.; Tsang, D. C. W.; Rinklebe, J.; Hou, D. Sulfur-Modified Biochar as a Soil Amendment to Stabilize Mercury Pollution: An Accelerated Simulation of Long-Term Aging Effects. *Environ Pollut.* 2020, *264*, 114687. DOI: 10.1016/j.envpol.2020.114687.

[119] O'Connor, D.; Peng, T.; Li, G.; Wang, S.; Duan, L.; Mulder, J.; Cornelissen, G.; Cheng, Z.; Yang, S.; Hou, D. Sulfur-Modified Rice Husk Biochar: A Green Method for the Remediation of Mercury Contaminated Soil. *Sci. Total Environ.* 2018, *621*, 819–826. DOI: 10.1016/j.scitotenv.2017.11.213.

[120] Hu, H.; Xi, B.; Tan, W. Effects of Sulfur-Rich Biochar Amendment on Microbial Methylation of Mercury in Rhizosphere Paddy Soil and Methylmercury Accumulation in Rice. *Environ. Pollut.* 2021, *286*, 117290. DOI: 10.1016/j.envpol.2021.117290.

[121] Elad, Y.; Cytryn, E.; Harel, Y. M.; Lew, B.; Graber, E. R. The Biochar Effect: Plant Resistance to Biotic Stresses. *Phytopathol. Mediterr.* 2011, *50*, 335–349. https://www.jstor.org/stable/26556455.

[122] Eser, A. Comparative Life Cycle Assessment of Renewable Activated Carbon Technologies. Master's Thesis, Faculty of Engineering and Natural Sciences, Tampere University, 2025. https://trepo.tuni.fi/bitstream/handle/10024/228448/EserAleyna.pdf?sequence=2&isAllowed=y.

[123] Mukherjee, A.; Okolie, J. A.; Niu, C.; Dalai, A. K. Techno-Economic Analysis of Activated Carbon Production from Spent Coffee Grounds: Comparative Evaluation of Different Production Routes. *Energy Convers. Manag. X* 2022, *14*, 100218. DOI: 10.1016/j.ecmx.2022.100218.

[124] Intratec. Calcium Carbonate Prices. Intratec Solutions LLC. n.d. https://www.intratec.us/solutions/primary-commodity-prices/commodity/calcium-carbonate-prices. (accessed May 4, 2026).

[125] Cavin Resource. Ammonia (NH_3) – Bulk Supply for Industrial and Agricultural Applications. n.d. https://cavinresource.com/product/liquid-ammonia-price-per-ton. (accessed May 4, 2026).

[126] Foodcom S.A. Magnesium Oxide (E530). n.d. https://foodcom.pl/en/products/magnesium-oxide/. (accessed May 4, 2026).

[127] Univar Solutions. Product Page 5096. n.d. https://www.univarsolutions.co.uk/5096. (accessed May 4, 2026),

[128] Univar Solutions. Product Page 1011720. n.d. https://www.univarsolutions.co.uk/1011720. (accessed May 4, 2026).

[129] Zhang, Q.; Niu, W. Q.; Du, Y. D.; Li, G. C.; Ma, L.; Cui, B. J.; Sun, J.; Niu, X. Y.; Siddique, K. H. M. Sustainable Effects of Nitrogen Reduction Combined with Biochar on Enhancing Maize Productivity and Nitrogen Utilization. *Eur. J. Agron.* 2025, *162*, 127429. DOI: 10.1016/j.eja.2024.127429.

[130] Poluszyńska, J.; Ślęzak, E.; Wieczorek, P. P. Biochar as an Agent Improving Soil Properties. *Przem. Chem.* 2019, *98*, 1000–1007. DOI: 10.15199/62.2019.1.15.

[131] European Biochar Certificate (EBC). European Biochar Certificate – Guidelines for a Sustainable Production of Biochar (Version 10.4). Carbon Standards International (CSI), 2024. http://european-biochar.org.

[132] Ranadev, P.; Revanna, A.; Bagyaraj, D. J.; Shinde, A. H. Sulfur Oxidizing Bacteria in Agro Ecosystem and Its Role in Plant Productivity—A Review. *J. Appl. Microbiol.* 2023, *134*(8), lxad161. DOI: 10.1093/jambio/lxad161.

[133] Zhang, Z.; Xuan, X.; Wang, J.; Zhao, X.; Yang, J.; Zhao, Y.; Qian, J.; Wang, T. Evolution of Elemental Nitrogen Involved in the Carbonization Mechanism and Product Features from Wet Biowaste. *Sci. Total Environ.* 2023, *884*, 163826. DOI: 10.1016/j.scitotenv.2023.163826.

[134] Greco, G.; Videgain, M.; Di Stasi, C.; Pires, E.; Manya, J. J. Importance of Pyrolysis Temperature and Pressure in the Concentration of Polycyclic Aromatic Hydrocarbons in Wood Waste-Derived Biochars. *J. Anal. Appl. Pyrolysis* 2021, *159*, 105337. DOI: 10.1016/j.jaap.2021.105337.

[135] Yadav, A.; Ansari, K. B.; Simha, P.; Gaikar, V. G.; Pandit, A. B. Vacuum Pyrolysed Biochar for Soil

Amendment. *Resour.-Eff. Technol.* 2016, *2*, S177–S185. DOI: 10.1016/j.reffit.2016.11.004.

[136] Mahari, W. A. W.; Nam, W. L.; Sonne, C.; Peng, W.; Phang, X. Y.; Liew, R. K.; Yek, P. N. Y.; Lee, X. Y.; Wen, O. W.; Show, P. L.; et al. Applying Microwave Vacuum Pyrolysis to Design Moisture Retention and pH Neutralizing Palm Kernel Shell Biochar for Mushroom Production. *Bioresour. Technol.* 2020, *312*, 123572. DOI: 10.1016/j.biortech.2020.123572.

[137] Sharma, G.; Dewangan, A. K.; Yadav, A. K.; Ahmad, A. Feasibility of Waste-to-Hydrogen Generation System Based on Gasification/Pyrolysis: A Comprehensive Review of Experimental Studies. *J. Therm. Anal. Calorim.* 2024, *149*(23), 13629–13651. DOI: 10.1007/s10973-024-13776-3.

[138] Nguyen, V. G.; Nguyen-Thi, T. X.; Nguyen, P. Q. P.; Agbulut, U.; Nguyen, L. H.; Balasubramanian, D.; Tarelko, W.; Bandh, S. A.; Pham, N. D. K. Recent Advances in Hydrogen Production from Biomass Waste with a Focus on Pyrolysis and Gasification. *Int. J. Hydrogen Energy* 2023, *54*, 127–160. DOI: 10.1016/j.ijhydene.2023.05.049.

[139] Cai, J.; Lin, N.; Li, Y.; Xue, J.; Li, F.; Wei, L.; Yu, M.; Zha, X.; Li, W. Research on the Application of Catalytic Materials in Biomass Pyrolysis. *J. Anal. Appl. Pyrolysis* 2024, *177*, 106321. DOI: 10.1016/j.jaap.2023.106321.

[140] Pilatau, A.; Czajka, K. M.; Filho, G. P.; Medeiros, H. S.; Kisiela, A. M. Evaluation Criteria for the Assessment of the Influence of Additives ($AlCl_3$ and $ZnCl_2$) on Pyrolysis of Sunflower Oil Cake. *Waste Biomass Valorization* 2017, *8*, 2595–2607. DOI: 10.1007/s12649-017-0021-z.

[141] Mishra, R. K.; Mohanty, K. Bio-Oil and Biochar Production Using Thermal and Catalytic Pyrolysis of Low-Value Waste Neem Seeds Over Low-Cost Catalysts: Effects of Operating Conditions on Product Yields and Studies of Physicochemical Characteristics of Bio-Oil and Biochar. *Biochar* 2021, *3*, 641–656. DOI: 10.1007/s42773-021-00105-2.